

# **Characteristics of Middle and Upper Tropospheric Clouds as Deduced from Rawinsonde Data**

by  
David O'C. Starr  
and  
Stephen K. Cox

Department of Atmospheric Science  
Colorado State University  
Fort Collins, Colorado



**Department of  
Atmospheric Science**

Paper No. 327

CHARACTERISTICS OF MIDDLE AND UPPER TROPOSPHERIC CLOUDS  
AS DEDUCED FROM RAWINSONDE DATA

by  
David O'C. Starr and Stephen K. Cox

Research supported by  
National Aeronautics and Space Administration  
Goddard Space Flight Center  
under grant NSG 5357

Department of Atmospheric Science  
Colorado State University  
Fort Collins, Colorado

November , 1980

Atmospheric Science Paper Number 327

## ABSTRACT

This study characterizes the static environment of middle and upper tropospheric clouds as deduced from rawinsonde data from 24 locations in the contiguous U.S. for 1977. Computed relative humidity with respect to ice is used to diagnose the presence of cloud layer. The deduced seasonal mean cloud cover estimates based on this technique are shown to be reasonable. Over 3600 cloud cases qualified for the analysis. The cases are stratified by season and pressure thickness, i.e. thick and thin. The dry static stability, vertical wind speed shear and Richardson number are computed for three layers for each case, i.e. the sub-cloud and above cloud layers and an in-cloud layer bounded by the cloud-top level. Mean values for each parameter and, in some instances, the corresponding relative frequency distributions are presented for each stratification and layer. The relative frequency of occurrence of various structures is presented for each stratification, e.g. increasing static stability with height through the three layers.

The observed values of each parameter vary over quite large ranges for each layer. The observed structure of each parameter for the layers of a given case is also quite variable. Structures corresponding to any of a number of different conceptual models, which are reviewed, may be found though some are substantially more common than others. It is of note that moist adiabatic conditions are not commonly observed and that the stratification based on thickness yields substantially different results for each group. Summaries of the results are included in the text.

## ACKNOWLEDGMENTS

The authors gratefully acknowledge the support of the computing facility at the National Center for Atmospheric Research, which is sponsored by the National Science Foundation. The primary support for this research was provided by the National Aeronautics and Space Administration under a climate-related grant administered by the Goddard Space Flight Center, under grant NSG 5357.

## TABLE OF CONTENTS

	<u>PAGE</u>
ABSTRACT	i
ACKNOWLEDGMENTS	11
TABLE OF CONTENTS	iii
1. INTRODUCTION	1
2. DATA ANALYSIS METHODOLOGY	4
2.1 Brief Review of Conceptual Models	4
2.2 The Basic Data Set	8
2.3 Data Processing and Analysis Procedures	9
2.4 Rawinsonde Observed Relative Humidity and Cloud Cover	18
2.5 The Cloud Case Data Set	22
3. RESULTS	25
3.1 Static Stability	25
3.1.a Mean Stability Structures	25
3.1.b Relative Frequency of Various Stability Structures	30
3.1.b.i Thick Cloud Cases	32
3.1.b.ii Thin Cloud Cases	38
3.1.c Relative Frequency Distributions of Stability	41
3.2 Vertical Wind Shear	47
3.3 Richardson Number	58
4. SUMMARY AND CONCLUSIONS	63
REFERENCES	69

## 1. INTRODUCTION

This study attempts to characterize certain aspects of the environment associated with middle and upper tropospheric stratiform clouds. The results will be utilized in the development of simple realistic models of the thermodynamic energy budgets of these cloud forms in a future study. The models will be used to investigate the role of various physical processes in the formation, maintenance and dissipation of these clouds. The motivation for studying these cloud forms is based on two factors. The first is that these clouds cover very extensive areas of the earth at any given time. Secondly, clouds are the most significant atmospheric constituent affecting the distribution of radiative energy loss or gain in the earth-atmosphere system. In other words, relative changes in cloud cover or cloud optical depth within a typical atmospheric column may lead to larger changes, both in the vertical distribution of net radiative energy gain within that column and in the corresponding surface radiative budget, than do similar relative changes in the concentration of any other constituent, (e.g. Starr, 1976). Middle and upper tropospheric clouds tend to more substantially alter the vertical distribution of net radiative energy gain than low level clouds, (e.g. Starr, 1976). The horizontal and vertical gradients of the net radiation budget comprise the basic forcing function governing the general circulation of the atmosphere.

Much attention has been focused on the simulation of the general circulation and climate modelling in recent years, (e.g. U.S. Committee for the GARP, 1978). A number of general circulation models have been developed by various groups, (see reviews by ISCU, 1974 and Starr and Cox, 1977). The

sensitivity of such models to variations in both the prescription of radiatively active constituents and radiative boundary conditions and in the formulation of the specific radiative scheme is well documented, e.g. Stone and Manabe, 1968; Washington, 1971; Schneider, 1975, Fels and Kaplan, 1975; Schneider et al., 1978. Numerous simple energy balance climate models have also been developed, e.g. Budyko, 1969; Sellers, 1969. The model simulations of mean climate state and its variability are also quite sensitive to the radiative component, e.g. Budyko, 1969; Sellers, 1969; Warren and Schneider, 1979; Coakley, 1979. Based upon the above studies, it is expected that the method of incorporating the effects of middle and upper tropospheric cloud forms into the climate simulations has a significant effect on the results. However, the methods of incorporating the effects of stratiform clouds in these models are generally of a very simple nature. The least complex methods utilize estimates of mean climatological cloudiness and coarse estimates of mean cloud radiative properties to prescribe these factors for the radiative component of the model. The most sophisticated methods utilize the model predicted relative humidity to predict the cloud cover but still employ estimates of mean radiative properties. The method of predicting stratiform cloud cover is generally based on an empirically derived linear relationship between relative humidity and cloud cover. Typically, the relationship used is similar to that reported by Smagorinsky, (1960), which was based on analysis of synoptic data. A requirement for sufficiently large and positive, model predicted, large-scale vertical velocity is also typically used to constrain the diagnosis of cloud cover.

The reason for utilizing such simple methods for the diagnosis of cloud cover and cloud properties in these models is two-fold. First, simplicity is highly desirable in order to minimize the computational requirements for the simulations. This is particularly true for the general circulation models. The limited computational capability available for model simulations dictates the use of parametric diagnosis of stratiform cloudiness, since the horizontal and vertical resolution of the models is limited. Secondly and more importantly, quantitative information on both the actual areal extent and variability of such clouds and their associated radiative properties in the atmosphere is sparse. Possible relationships between these quantities and other observable atmospheric parameters are even less well-known. On a more fundamental level, the basic physics of these clouds is not well understood. Relationships between the role of various physical processes and the physical environment in which they act have not been quantitatively assessed in any universal sense though a few limited case studies have been reported, e.g. Heymsfield, 1977. These issues have been addressed in the report of the JOC AD HOC Working Group on activation of the STRATEX Programme (7 January 1977). The aim of this study is to provide quantitative information which will aid in achieving a better understanding of the atmospheric environment associated with these cloud forms, the role of various physical processes in the life-cycle of these clouds, and their areal extent.



## 2. DATA ANALYSIS METHODOLOGY

By utilizing synoptic scale rawinsonde data this study investigates the static stability and the vertical wind shear associated with middle and upper tropospheric clouds. In this way the relative applicability of a number of simple conceptual models may be assessed. These conceptual models are summarized below.

### 2.1 Brief Review of Conceptual Models

The classical view of the environment associated with these cloud forms is depicted in Figure 1. In this view, the clouds are formed in an upgliding air mass above an elevated frontal zone. Vertical motion is positive above the frontal surface and negative below it. Adiabatic cooling due to lifting of the air mass is responsible for the existence of large-scale saturation. The stability of the cloud layer is determined by its pre-condensation stability and the amount of lifting. Sufficient lifting of a layer, which is initially only moderately stable, will produce unstable conditions. Once an unstable layer is produced, the tendency is for this layer to deepen, especially if the lifting persists. Since the vertical motion in the lifted air mass is greatest near the frontal zone, the cloud layer will generally form just above the front. Thus, the cloud layer is bounded below by a very stable layer. If unstable conditions are achieved, then vertical convective circulations may develop as in altocumulus clouds. These circulations are generally presumed to be weak, though Heymsfield (1977) reports that this may not always be the case. Strong vertical shear of the horizontal wind is anticipated across the frontal zone

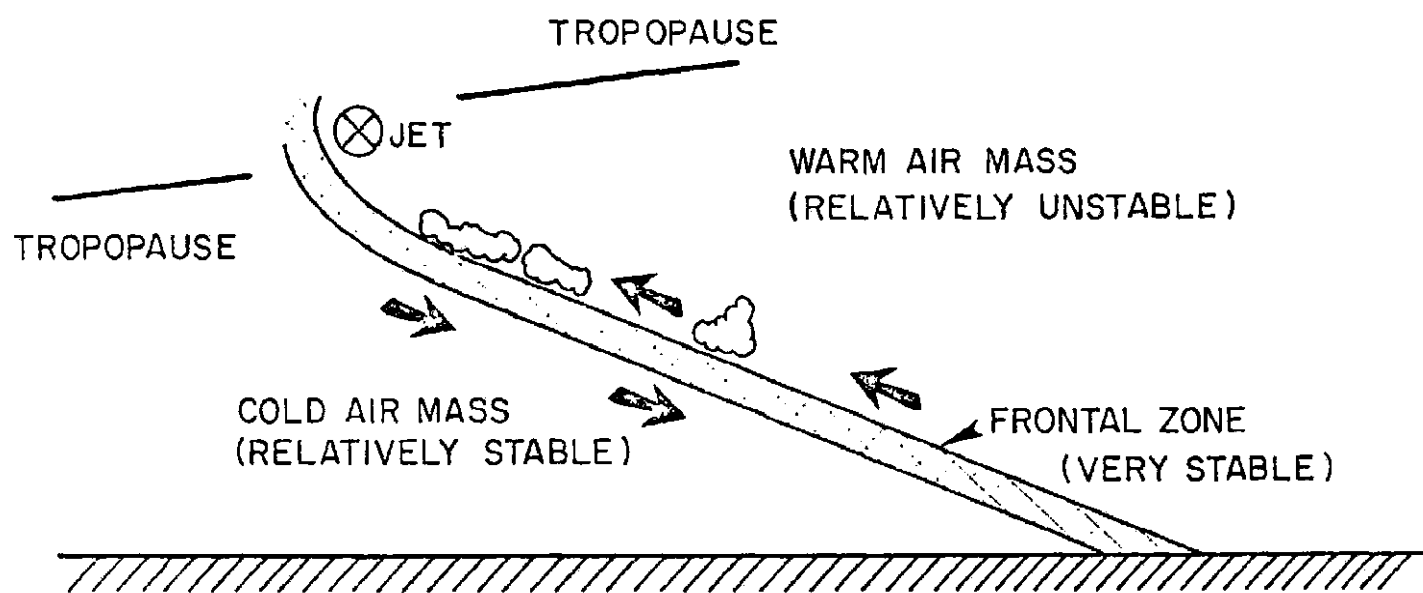


Figure 1. Classical model of the environment associated with middle and upper tropospheric clouds. Arrows indicate air motion relative to the front.

below the cloud layer. This was found in a study by Reuss (1967) of cirrus bands formed along frontal surfaces.

Another viewpoint may be found in the observations reported by Ludlam (1947, 1956), Oddie (1959), Yagi (1969), and Heymsfield (1975a,b). These studies report on the atmospheric environment associated with a few cirrus uncinus cloud cases. A very unstable layer, i.e. an approximately dry adiabatic lapse rate, is associated with the formation of a cloud head. A stable, capping layer, which may correspond to a frontal zone is sometimes observed. However, there is some disagreement about this being a universal feature. Another stable layer bounds the formative region from below, and again, there is disagreement about the stability of this layer. Heymsfield's observations show this layer to be very stable, while Yagi's observations show it to be slightly more stable than the formative zone. Thus, in one instance, the environmental conditions may correspond to the classical view, except possibly for the stable capping layer, while in another the presence of a sub-cloud frontal zone is not indicated. Heymsfield points out that vertical shear of the horizontal wind speed appears to be important in the formation of these clouds, though either positive or negative shear may be present. Heymsfield also notes that the local vertical motion field responsible for the formation of the cloud may be due to wave motion, i.e. gravity waves, originating in the bounding stable layer. If this is correct, then large-scale vertical lifting may not be required for cloud layers to form. There is also some question as to the origin of these structures.

It is also possible that in the later stages of the life-cycle of an elevated frontal zone, when its stability has been diminished by

diffusion and turbulence, that simple mixing across the front of warmer, moist air from above and cooler, not too dry air from below may lead to saturation and condensation. This would be somewhat analogous to the formation of radiation fog. Both vertical shear and stability would tend to be maximized within the cloud layer relative to conditions above or below the cloud. No large-scale lifting would be required.

Persistence of clouds formed by outflow from deep convection may also be responsible for the existence of extensive cloud layers. This may be readily observed in satellite photos. In this instance, large-scale uplift may not be involved in the maintenance of the cloud. There is probably a strong tendency for a stable capping layer since such a feature could play a role in initiating the outflow.

Upper level stratiform clouds are not always directly associated with frontal discontinuities. Orographic cloud forms are a prime example, (e.g. Ludlam, 1956). In this case, the vertical motion field is not due to large-scale uplift but to the flow adjusting to an impedance below. Condensation brought about by adiabatic cooling destabilizes the region about cloud base and stabilizes the region above cloud top, relative to the situation at these levels before lifting. The stability of the internal portions of the cloud layer is a function of the pre-lifted stability and the amount of lifting, i.e. larger amplitude waves produce greater instability. Quite large vertical shears may be associated with the region below the cloud layer as indicated by the presence in many instances, of extreme turbulence and rotor clouds in this region. Another example may be the jet stream cirrus. Although in some instances, these clouds are

undoubtedly associated with the elevated frontal zones coupled with jet streams, Conover (1960) suggests that they may be driven by vertical circulations arising from horizontal vortices due to the jet flow. Though the cloud patterns are observed to closely parallel temperature discontinuities, which are probably associated with old fronts, in some cases they are observed to exist well above these discontinuities. The tropopause may act as a stable capping layer for these clouds. The magnitude of the vertical shear of the horizontal wind should be a minimum near the region of cloud top.

Clouds do form in a lifted air mass well above the frontal zone. This is substantiated not only by Conover's observations, but also by the commonly observed growth of jet contrails into cirrus layers. Thus, lifting may produce saturation well away from the front. Heymsfield (1977) has noted that local upward vertical velocities play a large role in the formation of these clouds. However, since the lifting is weak away from the front, and the jet induced vortical circulations may not always be present, it may be hypothesized that clouds of these types form in layers where the air was initially somewhat unstable so that convective currents might form.

One feature of all the stratiform clouds, which is universal, is that condensation acts to destabilize the region about cloud base and stabilize the region above cloud top.

## 2.2 The Basic Data Set

For these analyses, rawinsonde data from 24 continental U.S. stations for the year 1977 were used. The stations were chosen so that a roughly uniform geographical distribution over the continental

U.S. between  $30^{\circ}$  N and  $50^{\circ}$  N latitude was obtained. These stations are depicted in Figure 2. Only 0000 and 1200 GMT sondes were used. Thus, the total basic data set is comprised of  $\sim 17,500$  sondes. The National Center for Atmospheric Research provided the basic rawinsonde data on mass storage for easy access by computer. The data from a particular sonde are comprised of the temperature, relative humidity, geopotential height, wind direction and wind speed at various pressure levels. All standard pressure levels, i.e. 50 mb resolution, and all significant levels are included in the basic rawinsonde data. For this data set, the mean vertical resolution is  $\sim 30$  mb for the domain of interest, i.e. surface level up to the 200 mb level.

### 2.3 Data Processing and Analysis Procedures

For the purposes of these analyses, an atmospheric layer, which is saturated with respect to ice, is taken to be a cloud layer. The justification for this assumption is given in the following section. At that point, the validity of utilizing rawinsonde measured relative humidity for these analyses is also assessed.

The basic data set was divided into seasons. In this study, the summer season corresponds to the months of June, July and August; the fall season corresponds to the months of September, October and November; the winter season corresponds to the months of December, January and February; and the spring season corresponds to the months of March, April and May. All data for each season for all stations were grouped together, i.e. no regional analysis or time of day distinctions were attempted. Regional characteristics of the overall data set will be addressed in a future study already in progress. Each

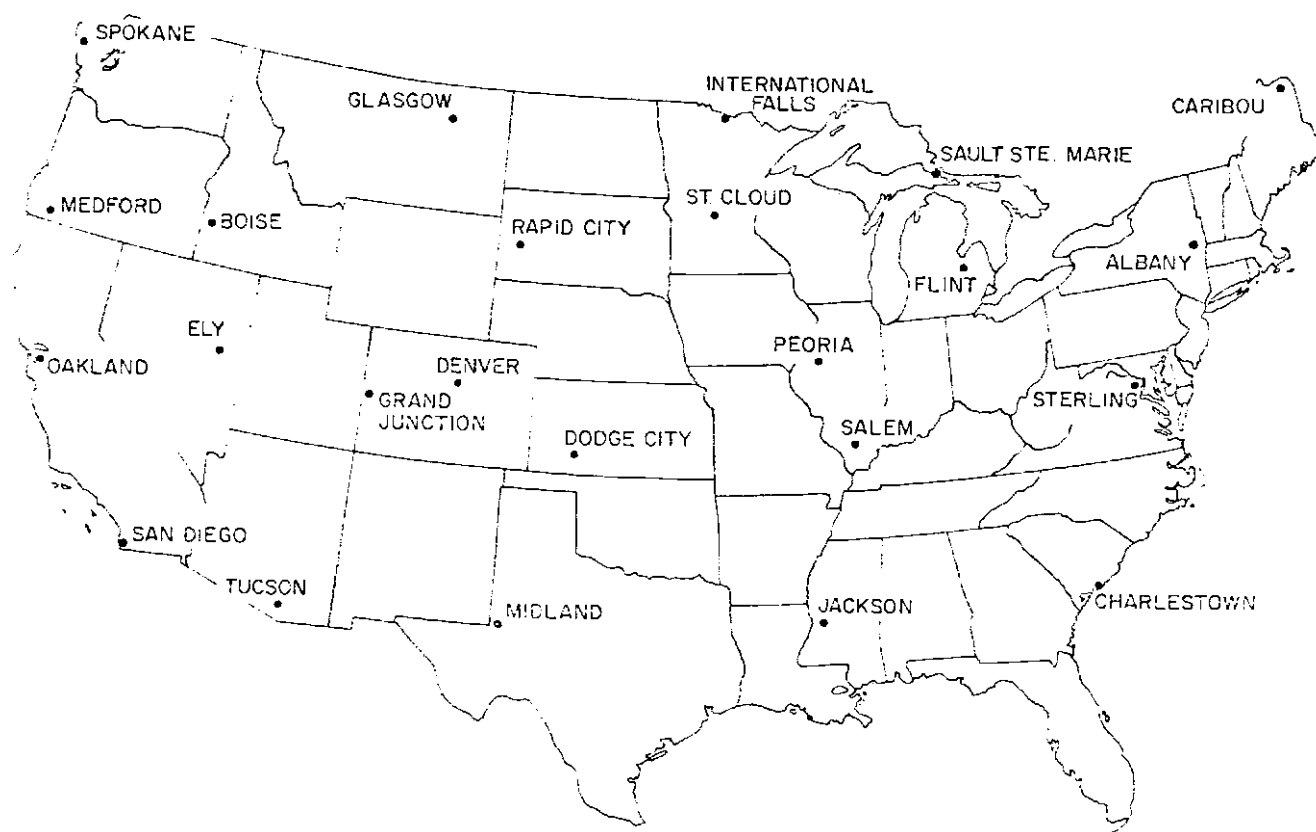


Figure 2. Geographical distribution of National Weather Service rawinsonde stations used for this study.

sonde in a seasonal group was considered to determine if a cloud layer was present.

For these analyses, only data at pressures less than or equal to 500 mb were considered. There is one exception to this, which will be noted later. In addition, only data at pressures less than the lowest pressure having a temperature greater than  $0^{\circ}$  C were considered. Thus, this study is limited to high level clouds, which are predominantly ice-phase. Relative humidity data at temperatures less than  $-40^{\circ}$  C do not exist in the basic data set. The analysis for a particular sonde was terminated at this level.

List (1966) presents values for the ratio of the saturation water vapor pressure with respect to water to the saturation vapor pressure with respect to ice as a function of temperature,  $T$ . These data are a good approximation to the ratio of the relative humidity with respect to ice,  $RH_i$ , to the relative humidity with respect to water,  $RH_w$ . The data were fit with a second order polynomial. These data and the polynomial fit are presented in Figure 3. At each data level considered, this polynomial was used to compute the relative humidity with respect to ice from the observed temperature and relative humidity. Note that the observed relative humidity is referenced to water and that the data being considered correspond to temperatures between  $0^{\circ}$  C and  $-40^{\circ}$  C.

For each sonde, all data levels in the pressure and temperature domain noted above, were searched for saturation with respect to ice, i.e.  $RH_i \geq 100\%$ . Any saturated layer was denoted as a cloud layer. If only one saturated level was found, it was still considered to be a cloud layer. If saturation was found at the lowest data level in the analysis domain, the analysis domain was extended in order to locate



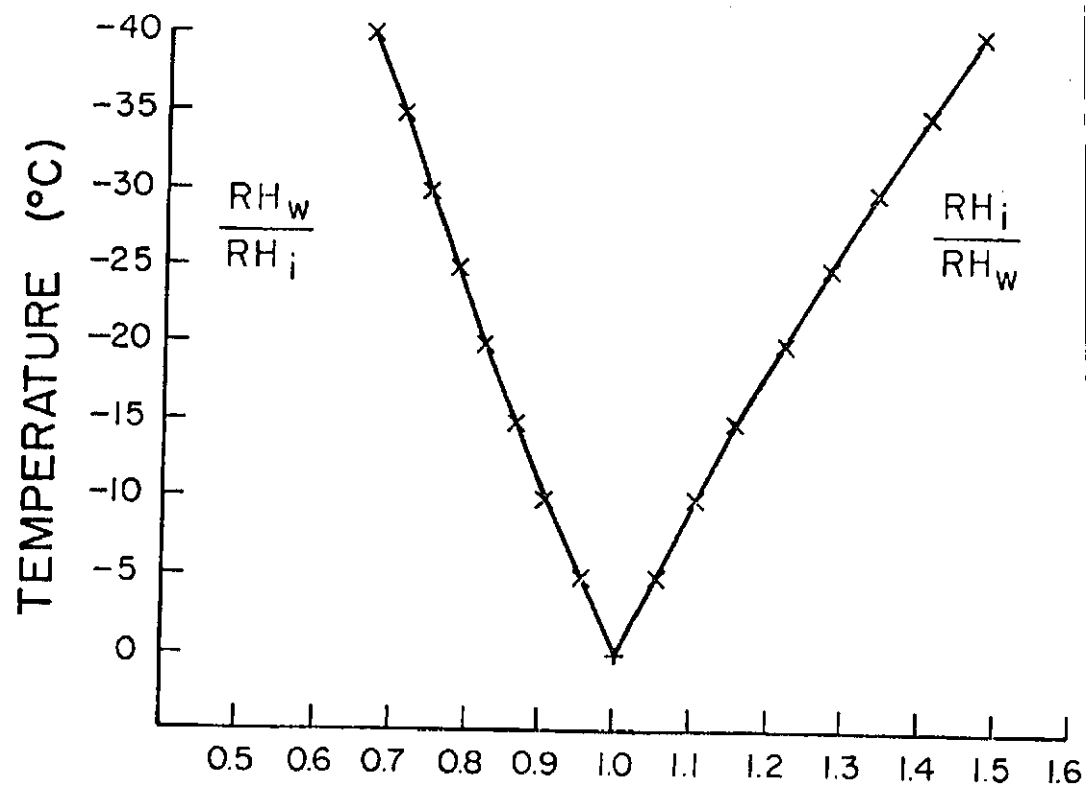


Figure 3. Plotted points represent the ratio of the saturation water vapor pressure with respect to a water surface to the saturation water vapor pressure with respect to an ice surface as a function of temperature (after List, 1966). The plotted curves correspond to the approximation employed in this study for the ratio of relative humidity with respect to ice to relative humidity with respect to water, i.e.  $RH_i / RH_w$ , and its inverse.

cloud base, i.e. the lowest saturated level below the 500 mb or  $0^{\circ}$  C level without any intervening unsaturated levels. If positive temperatures were encountered in the attempt to locate cloud base, then the observed values of  $RH_w$  were used to test for saturation, i.e.  $RH_w \geq 100\%$  for  $T > 0^{\circ}$  C.

When a cloud layer was determined to be present, three layers were defined for these analyses. They are the over-cloud layer, the cloud-top layer and the sub-cloud layer. The over-cloud layer is defined by the uppermost saturated level and the next higher level, which is unsaturated. The cloud-top layer is defined by the uppermost saturated level and the next lower level, which may not be saturated if only one saturated level was encountered. In most cases, at least two adjacent saturated levels were found. Note that the over-cloud layer and the cloud-top layer share a common boundary. The sub-cloud layer is defined by the lowest level at which saturation is found, i.e. no intervening unsaturated levels between this level and the cloud-top level, and the next lower level, which is unsaturated. However, in the case of a cloud layer which is defined by only one saturated level, the sub-cloud layer is defined to be the layer adjacent to and below the cloud-top layer. If any data were missing, i.e.  $T$ ,  $RH_w$ , height, wind direction or wind speed, for the levels needed to define these layers, the case was eliminated from the analyses. For each of these three layers, three quantities were computed, namely: the dry static stability, the vertical shear of the horizontal wind speed and the atmospheric analog of the Richardson number.

Dry static stability,  $\sigma$ , corresponds to the vertical derivative of potential temperature,  $\theta$ , i.e.

$$\sigma \equiv \frac{\partial \theta}{\partial z} \quad (2.1)$$

where  $z$  is the height. The potential temperature is given by Poisson's equation:

$$\sigma \equiv T \left( \frac{P}{P_0} \right)^{-k}$$

where  $P$  is the pressure,  $P_0$  is a constant reference pressure and  $k$  is a constant. Equation (2.1) was evaluated for a given layer as:

$$\sigma = (\tau_d - \tau) \left( \frac{\bar{P}}{P_0} \right)^{-k} \quad (2.2)$$

where  $\tau$  is the temperature lapse rate for the layer,  $\tau_d$  is the dry adiabatic lapse rate and  $\bar{P}$  is the mean layer pressure. If the upper level of a layer is denoted as the  $n^{\text{th}}$  level and the lower level of a layer is denoted as the  $(n-1)^{\text{th}}$  level, the formulae used to evaluate Eqn. (2.2) are:

$$\tau = \frac{(T_{n-1} - T_n)}{z_n - z_{n-1}}$$

and

$$\bar{P} = \frac{(P_n + P_{n-1})}{2}$$

where

$$\tau_d \equiv \frac{g}{c_p} = 9.8^\circ\text{K/km},$$

$$P_0 = 1000 \text{ mb}$$

and

$$k \equiv \frac{R_g}{c_p} = \mathbf{0.288}$$

where  $g$  is the acceleration due to gravity,  $C_p$  is the specific heat of dry air at constant pressure and  $R_g$  is the real gas constant for dry air. The dry static stability is a measure of the stability of parcels within a layer to small vertical displacements. It quantifies the potential buoyancy force acting on a parcel. A more accurate measure of the stability might be obtained by also considering the vertical derivative of equivalent potential temperature,  $\theta_e$ , (e.g. Hess, 1959). However, for the temperature domain of this data set with its correspondingly small values of the saturation vapor pressure,  $\theta_e$  very nearly equals  $\theta$ . Thus, dry static stability is a good approximation to the stability in this domain.

The vertical shear of the horizontal wind speed,  $S$ , for a layer was computed as:

$$S = \frac{|\tilde{v}_n| - |v_{n-1}|}{z_n - z_{n-1}} \quad (2.3)$$

where  $|\tilde{v}_n|$  is the horizontal wind speed at pressure level  $n$ . Wind direction has been ignored for the consideration of vertical wind shear in this study. A number of detailed case studies of extensive altostratus and cirrostratus cloud layers by one of the authors led to the conclusion that directional shear is generally small even in

the vicinity of elevated fronts associated with the cloud layers considered; It is for this reason because of a desire for simplicity in the analyses that wind direction is not considered here.

The Richardson number,  $R$ , for a layer was computed as:

$$R = \frac{g\sigma}{\bar{\theta} s^2} \quad (2.4)$$

where the mean layer potential temperature is given by:

$$\bar{\theta} = \frac{(T_n + T_{n-1})}{2.0} \left( \frac{\bar{P}}{P_0} \right)^{-k}$$

The Richardson number is a non-dimensional number, which corresponds to a ratio of the buoyancy forces to the mechanical forces, i.e. shear stress, acting on a parcel. It is a measure of the production and dissipation of turbulent kinetic energy. Large values of  $R$  imply that turbulent kinetic energy is quickly damped, i.e. dissipated, in the mean flow. Small values of  $R$ , i.e.  $R \leq \sim 0.25$ , imply that the turbulent kinetic energy imbedded in the mean flow is maintained by the mean flow, i.e. production is greater than or equal to dissipation. Clear air turbulence occurs when a small Richardson number is observed for the mean flow.

We chose to analyze these parameters for a number of reasons. First, they are easy to compute and readily accessible from the basic data set. Second, they enable the identification of typical atmospheric structures, which may be associated with these cloud forms,

e.g. frontal zones, on an automated basis. This eliminates the need to analyze weather maps, which would greatly increase the difficulty and time required to accomplish a survey as extensive as this one. Third, they characterize the static environment associated with these layers. Note that the importance of horizontal advective processes in the life-cycle is currently being evaluated with this data set. Fourth, knowledge of the typical static stability structure associated with cloud forms is very useful in the design of simple thermodynamic budget models of stratified cloud layers, e.g. Schubert (1976) and Albrecht, et al (1979). Also, information on the turbulent kinetic energy budget of a cloud layer is important for design and closure of parametric models of convective energy transports within a layer.

For each layer for each season, frequency distributions were obtained for each parameter. Mean values and standard deviations were also computed. Structure information was compiled based on comparison of the values for each layer of a particular cloud case. Many different stratifications of the cloud case data set were attempted. Most turned out to be not very useful. However, stratifying the data on the basis of thickness of the cloud layer did provide some interesting results. Thin cloud layers were defined to be less than or equal to 50 mb thick, otherwise the cloud case was regarded as a thick cloud layer. The 50 mb thickness criterion was chosen because this is the minimum resolution of the basic data set and because it was felt that it might adequately discriminate between the fair weather thin cirrus and the strongly forced deep clouds associated with cyclones. In this way, it was hoped to distinguish between cases which might best correspond to the classical model and those which might best be described

by other conceptual models. The results of these analyses are presented in Section 3.

#### 2.4 Rawinsonde Observed Relative Humidity and Cloud Cover

In this section, the validity of utilizing relative humidity data from standard rawinsondes for the diagnosis of cloud layers is considered.

Humidity data from standard National Weather Service rawinsondes for ambient temperatures in the range of 0° C to -40° C are commonly regarded as having large inherent errors, especially at the colder temperatures. However, substantial improvements in the basic design of the sonde and the humidity element itself have been made in recent years. Reports by Brousaides (1973) and Brousaides and Morrissey (1974), hereafter referred to as MB, present a synopsis of potential errors in the redesigned sonde. This sonde has been in use since ~1973 at the National Weather Service launch sites in the U.S. Errors due to solar insolation and thermal lag have been substantially reduced compared to older sondes. However, the remaining errors are still substantial. Brousaides (1973) notes that the reproducibility, i.e. the relative precision, of the humidity sensors is within a range of approximately 6-7% in measured relative humidity. Except in the situation of heavy precipitation, washout was not found to be a severe problem for the new sonde. MB state that errors due to thermal lag are on the order of 6 to 9% in measured relative humidity, while solar insolation induced errors amount to 9 to 14% in the temperature and pressure domain considered in this study. However, for the geographic and height domain of this study and the 0000 and 1200 GMT launch times, solar insolation problems should be minimal, i.e. only ~25% of the sondes considered in this study potentially experienced direct solar exposure at some time during their

flight at solar elevations corresponding to greater than one hour above the horizon. Even these sondes were typically exposed at relatively small solar elevations. MB note that the rectification of flight data is very difficult due to the variability of the error sources, i.e. solar elevation, cloud conditions, previous thermal and humidity history, etc. This is especially true for standardized data sets, which are used in this study, where the complete minute-by-minute data record is unavailable. Correction of the basic data set employing their formulae was not attempted.

The data were tested for humidity lag. Data and formulae presented in Brousaides (1973) were used to formulate a test criterion of maximum observable response rate. Approximately 5% of the basic data set was tested against this criterion. The sample was random except that humidity was required to increase from the next lower level to the test level. An observed rate of change of humidity equal to or greater than 80% of the maximum observable response rate was found at less than 3% of the levels tested. Thus, in the basic data set, vertical gradients of humidity are rarely large enough to exceed the sensor capability.

Rhea (1978) has found the new sonde to be acceptable for locating cloud layers. Surface observations of cloud layers were compared to relative humidity with respect to ice computed from rawinsonde data for western Colorado. Saturated layers were found to correspond well with observations of cloud layers. Much improvement in this regard was noted, when compared to the last two generations of sondes.



Similar results were found by these authors. A number of case studies of the large-scale energy budgets associated with upper level stratiform cloud layers are in progress by these authors. The purpose of these studies is to try to ascertain the nature of the advective components of the budgets and the corresponding synoptic situation. Surface and satellite observations of cloud layers agreed quite well with deductions based solely on observed relative humidity with respect to ice. Probably the best validation for using post-1973 rawinsonde data to assess the presence of cloud layers may be found by considering the following. The percentage of sondes exhibiting saturation with respect to ice at pressures less than 600 mb and temperatures between 0° C and -40° C for the basic data set are given below for two latitude bands.

	Summer	Fall	Winter	Spring	Annual
30° N - 40° N	26.6	26.3	31.7	30.5	28.8
	(27.1)	(32.7)	(31.4)	(38.0)	(32.3)
40° N - 50° N	39.0	36.1	42.4	40.1	36.9
	(36.1)	(40.7)	(39.1)	(43.4)	(39.8)

The percentages in parentheses are the mean zonal cloud cover for these latitudes in the northern hemisphere for the middle and upper troposphere, which were derived from data presented in London (1957). London's estimates were based upon surface observations of various cloud forms. The effects of obscuration due to overlap of cloud layers were taken into account in deriving the estimates of cloud cover for the various cloud types presented in London (1957). The percentages given above were computed by summing the given cloud amounts for cirrus, altostratus, nimbostratus and cumulonimbus clouds and then

correcting these sums for overlap. The overlap correction consisted of assuming random distribution of cirrus, altostratus and nimbostratus clouds. Thus, the corrected sums are less than the uncorrected sums.

If saturation with respect to ice determined from rawinsonde data is a good indicator of the presence of a cloud, then for a large data sample, the percentage of sondes exhibiting saturation should correspond to the observed mean middle and upper tropospheric cloud cover. The agreement between seasonal mean zonal cloud cover estimated from surface observations and that based on analysis of rawinsonde data is fairly good. Exact agreement would not be anticipated for a number of reasons. First, this analysis is based on data for the continental U.S. for the year 1977, while London's estimates are based on other years for the entire northern hemisphere in these latitude bands. Thus, year-to-year variability in the cloud cover for the middle and upper troposphere and longitudinal variations in that cloud cover could be sources of disagreement. Also, due to the  $-40^{\circ}$  C limit on the data sample for this analysis, some cirriform clouds cannot possibly be detected. In addition, some of the nimbostratus cloud forms may be too shallow or too warm to be detected by this analysis. This would be particularly true in the warmer seasons. Thus, the seasonal mean zonal cloud cover for the middle and upper troposphere derived from this analysis should be less than that actually observed even if the technique is valid. A compensating effect is that layers, which are saturated with respect to ice, are observed to be cloud free in some cases, e.g. Bigg and Meade (1971), Jayaweera and Ohtake (1972), and Detwiler and Vonnegut (1979). However, this situation occurs relatively infrequently (e.g. Lala, [1969]) reports that only 3% of the time is this

observed at Albany, New York) and normally at temperatures less than  $-30^{\circ}$  C. Since saturation with respect to ice at pressures less than 600 mb and temperatures between  $0^{\circ}$  C and  $-40^{\circ}$  C was detected in  $\sim 35\%$  of the sondes for Albany in 1977, less than 8% of the saturated layers determined by this analysis are anticipated to be cloud free. It is expected that errors arising from the limited vertical domain of this study are greater than those due to erroneous diagnosis. Therefore, the seasonal mean zonal cloud cover for the middle and upper troposphere derived here is likely to be less than that actually observed even if the technique is valid. It is of note that, except in winter, the estimated cloud cover derived in this study is less than that derived from London (1957) for both latitude bands.

## 2.5 The Cloud Case Data Set

Before discussing the results of the analyses of cloud characteristics, it is appropriate to consider the cloud case data set. In Table 1, the number of cloud cases, which qualified for these analyses on the basis of the criteria discussed in Section 2.3, are presented for each season for both cloud thickness groups. These are the number of cases for which the analyses of cloud layer characteristics were performed. In the following discussion of results, relative frequency of occurrence always refers to the percentage or fraction of the total number of cases in a particular group, i.e. season and thickness, exhibiting a particular characteristic. Many more thin cloud cases qualified for the analyses than thick cloud cases. This is partly because many of the thick saturated layers, which were found, were

saturated at the  $-40^{\circ}$  C level and, thus, were excluded from the analyses as cloud-top pressure could not be located.

	Summer	Fall	Winter	Spring	Total
Thick Clouds	189	251	246	200	886
Thin Clouds	863	765	524	564	2716
All Clouds	1052	1016	770	764	3602

Table 1. Number of cloud cases included in this study for each season and for each cloud thickness group.

In Figure 4, the relative frequency of occurrence of cloud cases with cloud-top pressure,  $P_{CT}$ , within 25 mb of a given pressure level is given for each season for both the thick cloud cases and the thin cloud cases. The corresponding mean cloud-top pressures are also noted. Mean cloud-top pressure is greatest in winter and least in summer. The shapes of the curves are highly influenced by the mean seasonal location of the  $-40^{\circ}$  C isotherm and its variation. The location of the mean seasonal tropopause and its variation also affect the shape of the curves. These two factors cause the observed diminishing relative frequencies above  $\sim 400$  mb. Note that the summer and fall curves are similar and that the spring and winter curves are similar for both thick and thin cloud cases. The mean cloud thickness is  $\sim 30$  mb for the thin cloud cases and nearly 150 mb for the thick cloud cases. However, only  $\sim \frac{1}{3}$  of the thick cloud cases are thicker than 150 mb. Thus, the mean is highly influenced by the very thick cases.

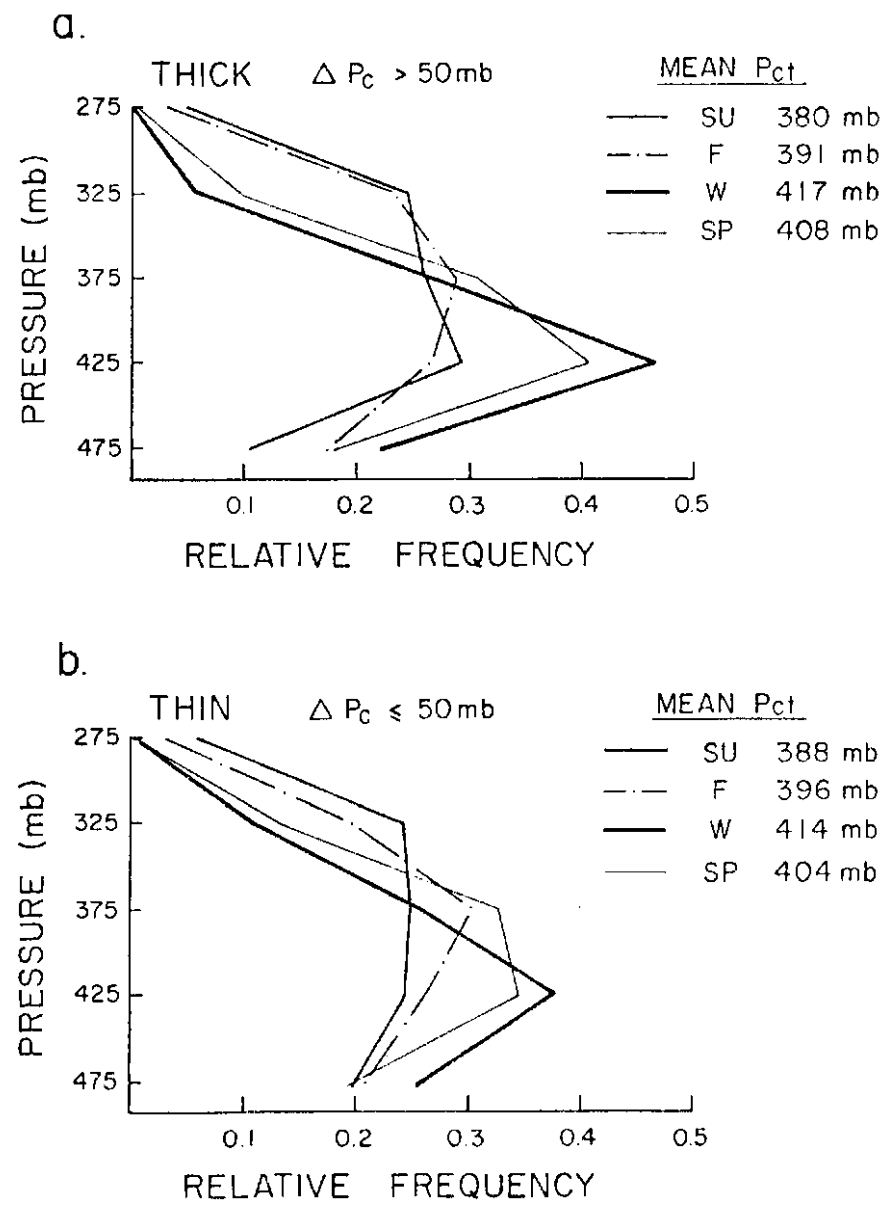


Figure 4. Relative frequency of occurrence for cloud canes with cloud top pressure,  $P_{ct}$ , within 25 mb of a given pressure for both (a) thick cloud cases and (b) thin cloud cases for each season. Seasonal mean cloud top pressures are also given.

### 3. RESULTS

#### 3.1 Stability

##### 3.1.a Mean Stability Structures

The results of the analyses of the dry static stability in the cloud-top layer,  $\sigma_T$ ; the over-cloud layer,  $\sigma_0$ ; and the sub-cloud layer,  $\sigma_S$ , are presented in this section. The seasonal means for the three layers, i.e.  $\overline{\sigma_T}$ ,  $\overline{\sigma_0}$ , and  $\overline{\sigma_S}$ , are given in Figure 5a for the thick cloud cases and in Figure 5b for the thin cloud cases. The seasonal means for the 350 mb to 450 mb layer,  $\overline{\sigma_4}$ , and for the 650 mb to 750 mb layer,  $\overline{\sigma_7}$ , computed from all sondes are included in each figure for comparison.

Comparing the  $\overline{\sigma_4}$ , and  $\overline{\sigma_7}$  curves, dry static stability is seen to decrease with increasing height in all seasons. The seasonal range of  $\overline{\sigma_4}$  is only  $0.36^\circ$  K/km with relative maxima, i.e. more stable, occurring in summer and winter. The winter maximum may be partly due to the inclusion of some cases, where the tropopause is within the 350 mb to 450 mb layer. This may occur when a deep, cold trough is located over a station at launch time and would lead to a more stable value of  $\overline{\sigma_4}$ . The seasonal range of  $\overline{\sigma_7}$  is nearly  $1.5^\circ$  K/km. Thus, the middle troposphere undergoes a much larger seasonal variation of mean dry static stability, when compared to the upper troposphere. The winter season is the most stable and the summer season is the most unstable at the 700 mb level. In terms of  $\overline{\sigma_7}$ , spring resembles summer and fall is intermediate between winter and summer. The seasonal behavior of  $\overline{\sigma_7}$  may be partly attributed to the increased frequency and strength of elevated fronts occurring the the 650 mb to 750 mb layer during the cold seasons. Stabilization of the lower troposphere due to infrared

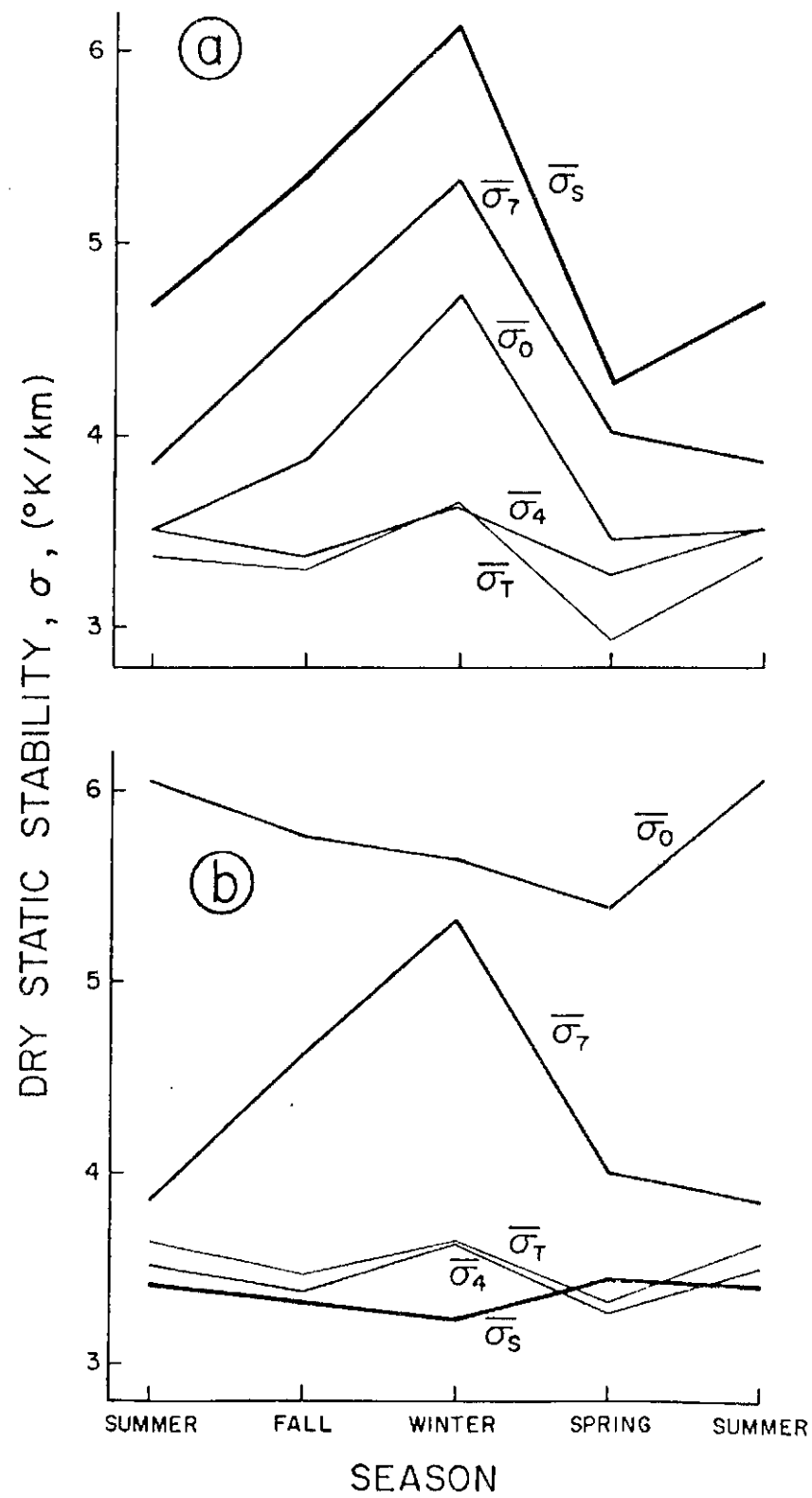


Figure 5. Seasonal mean dry static stability for the cloud-top layer,  $\overline{\sigma}_T$ ; the over-cloud layer,  $\overline{\sigma}_0$ ; and the sub-cloud layer,  $\overline{\sigma}_s$ , for (a) thick cloud cases and (b) thin cloud cases. Mean seasonal dry static stability at 400 mb,  $\overline{\sigma}_4$ , and at 700 mb,  $\overline{\sigma}_7$ , are included for comparison. See text for further explanation.

radiative processes acting at night may also play a role in raising  $\overline{\sigma_7}$  in the winter, especially at the high elevation stations. Also, enhanced convective mixing in summer may play a role in lowering  $\overline{\sigma_7}$  in that season. If only sondes exhibiting saturation with respect to ice at a level above the 500 mb level are used to compute  $\overline{\sigma_4}$  and  $\overline{\sigma_7}$ , the curves are altered somewhat. In this case,  $\overline{\sigma_7}$  is decreased by less than  $0.1^\circ$  K/km in each season, when compared to the plotted values. The values of  $\overline{\sigma_4}$  are increased by approximately  $0.1^\circ$  K/km in winter and spring and by  $0.3$  and  $0.2^\circ$  K/km in summer and fall, respectively. Thus, the mean difference in dry static stability between the upper and lower troposphere is less for cloud case sondes, when compared to all sondes. In summer, this difference is negligible for the cloud case sondes.

The observed values of  $\overline{\sigma_4}$  and  $\overline{\sigma_7}$  may be used to compute the seasonal mean rate of change of dry static stability with respect to pressure, i.e.  $(\overline{\sigma_7} - \overline{\sigma_4}) / 300$  mb. If this linear rate of change is assumed to be valid for the pressure domain considered here, the seasonal mean dry static stability at any pressure level in this domain may be computed as a linear function of that pressure. In order to compare the observed values of  $\overline{\sigma_T}$ ,  $\overline{\sigma_0}$ , and  $\overline{\sigma_S}$  to mean atmospheric conditions, "expected" mean values of  $\overline{\sigma_T}$ ,  $\overline{\sigma_0}$ , and  $\overline{\sigma_S}$  were computed from the observed respective mean mid-layer pressures by the above method. The assumption of linear decrease of  $\sigma$  with pressure should not have much effect on the computations of the "expected" mean values, since, except for the sub-cloud layer for the thick cloud cases, the mid-layer pressures occur predominantly in the 350 mb to 450 mb layer (see



Fig. 4). Thus, the expected mean values are based on small adjustments to the value of  $\overline{\sigma_4}$ .

Considering  $\overline{\sigma_T}$ ,  $\overline{\sigma_0}$ , and  $\overline{\sigma_S}$  for the thick cloud cases, the cloud-top layer is the most unstable layer and the sub-cloud layer is the most stable layer of the three in the mean for each season. The mean cloud-top layer is less stable than expected from mean conditions. The difference is nearly  $0.5^\circ$  K/km in spring,  $\sim 0.2^\circ$  K/km in winter, and  $\sim 0.1^\circ$  K/km in the other seasons. If the virtual dry static stability, i.e. using the moist adiabatic lapse rate instead of the dry adiabatic lapse rate in Eq. 2.2, is computed, the mean cloud-top layer is an additional  $\sim 0.5^\circ$  K/km more unstable than mean conditions. Therefore, it is primarily the moisture content of the mean cloud-top layer that distinguishes it from mean conditions in terms of stability to small vertical displacements.

The mean over-cloud layer for the thick cloud cases is more stable than expected from mean conditions by 0.1, 0.6, 1.1 and  $0.2^\circ$  K/km in summer, fall, winter and spring, respectively. The seasonal range of  $\overline{\sigma_0}$  is greater than that of  $\overline{\sigma_T}$  by a factor of  $\sim 3.5$ , which is surprising in that the mean difference between the mid-layer pressures is only  $\sim 30$  mb. The difference between  $\overline{\sigma_0}$  and  $\overline{\sigma_T}$  is 0.1, 0.6, 1.1 and  $0.5^\circ$  K/km in summer, fall, winter and spring, respectively. Thus, particularly in winter, the mean thick cloud layer is capped by a layer which is more stable than the cloud-top layer, even if differences in water vapor content are ignored.

The mean sub-cloud layer is the most stable layer and also exhibits the largest seasonal range in dry static stability of the three layers, which might have been anticipated from mean conditions, i.e.

$\overline{\sigma}_7$ . However, the observed values of  $\overline{\sigma}_S$  are greater than the values expected from mean conditions by approximately 1.1, 1.5, 1.8 and 0.7 ° K/km in summer, fall, winter and spring, respectively. These values suggest the presence of an elevated front in the sub-cloud layer. This may be seen by considering that in winter the value of  $\overline{\sigma}_S$  corresponds to a temperature lapse rate of only 4.7° K/km, which is absolutely stable even under saturated conditions at this pressure, i.e. ~550 mb.

Considering  $\overline{\sigma}_T$ ,  $\overline{\sigma}_0$ , and  $\overline{\sigma}_S$  for the thin cloud cases, the overcloud layer is observed to be the most stable of the three in the mean for each season, while the sub-cloud layer is the least stable except in spring. The observed values of  $\overline{\sigma}_T$  are greater than those expected from mean conditions by ~0.1° K/km in summer and fall, nearly equal in spring, and are less by ~0.2° K/km in winter. Thus, unlike the thick cloud cases, the mean cloud-top layer for the thin cloud cases tends to be slightly more stable than mean conditions. The seasonal range in  $\overline{\sigma}_T$  for the thin cloud cases is less than half that for the thick cloud cases, though the patterns are similar. The mean cloud-top layers for the thick and thin cloud cases are not that different in terms of dry static stability and in both cases it is primarily the water vapor content of the layers that distinguishes them from mean conditions.

The mean over-cloud layer for the thin cloud cases is more stable than expected from mean conditions by 2.6, 2.5, 2.0 and 2.2° K/km in summer, fall, winter and spring, respectively. These values suggest the presence of an elevated front above the thin cloud layer. In some cases, this stable layer is likely to correspond to the tropopause. The value of  $\overline{\sigma}_0$  in summer

corresponds to a temperature lapse rate of only  $\sim 5.4^\circ$  K/km, which is a very stable layer at this pressure level, ( $\sim 370$  mb). The seasonal range of  $\overline{\sigma_0}$  is much smaller for the thin cloud cases, when compared to the thick cloud cases, and the seasonal patterns are dissimilar, except that each exhibits a spring minimum. In each season, the mean over-cloud layer is much more stable for the thin cloud cases compared to the thick cloud cases even though the stability of the respective mean cloud-top layers is not too different.

Mean conditions suggest that for the thin cloud cases,  $\overline{\sigma_s}$  should be greater than  $\overline{\sigma_T}$ , however, this is not observed. The values of  $\overline{\sigma_s}$  are less than those expected from mean conditions by  $\sim 0.1^\circ$  K/km in spring and summer and  $\sim 0.2^\circ$  K/km in the other seasons. The stability of the mean sub-cloud layer is not too different from that of the mean cloud-top layer for the thin cloud cases. There is no indication of an elevated frontal zone in the mean sub-cloud layer for the thin cloud cases as there was for the thick cloud cases.

### 3.1.b. Relative Frequency of Various Stability Structures

Thus far, the mean stratification in terms of dry static stability in the vicinity of both thick and thin cloud layers have been quantified for each season. Differences in the mean dry static stability between the thin and thick cloud cases have been noted. However, the correspondence of the mean structures to the actual observed case by case structure must be established before any quantitative model of the typical stratification can be put forth, i.e. is the mean structure representative of the typical structure or is it the result of averaging multiple and different typical structures? In Table 2, the observed relative frequency of occurrence of various stratifications in

(a)

Thick Cloud Cases

	Su	F	W	Sp	Average
$\overline{\sigma_S}$ and $\overline{\sigma_0} \geq \overline{\sigma_T}$	27	34	34	27	30
$\overline{\sigma_S} < \overline{\sigma_T} \leq \overline{\sigma_0}$	11	11	12	12	11
$\overline{\sigma_S} \geq \overline{\sigma_T} > \overline{\sigma_0}$	35	35	34	34	35
$\overline{\sigma_S}$ and $\overline{\sigma_0} < \overline{\sigma_T}$	27	20	20	28	24
$\overline{\sigma_0} \geq \overline{\sigma_T}$	38	45	46	39	42
$\overline{\sigma_S} \geq \overline{\sigma_T}$	62	69	68	61	65

(b)

Thin Cloud Cases

	Su	F	W	Sp	Average
$\overline{\sigma_S}$ and $\overline{\sigma_0} \geq \overline{\sigma_T}$	43	40	38	41	41
$\overline{\sigma_S} < \overline{\sigma_T} \leq \overline{\sigma_0}$	21	17	21	17	19
$\overline{\sigma_S} \geq \overline{\sigma_T} > \overline{\sigma_0}$	14	16	17	17	16
$\overline{\sigma_S}$ and $\overline{\sigma_0} < \overline{\sigma_T}$	22	27	24	25	24
$\overline{\sigma_0} \geq \overline{\sigma_T}$	64	57	59	58	60
$\overline{\sigma_S} \geq \overline{\sigma_T}$	57	56	55	58	57

Table 2. Relative frequency of occurrence in percent of various stratifications of dry static stability among the overcloud layer,  $\overline{\sigma_0}$ ; the cloud-top layer,  $\overline{\sigma_T}$  and the sub-cloud layer,  $\overline{\sigma_S}$ , for each season and the "average" season for (a) thick cloud cases and for (b) thin cloud cases.

terms of dry static stability among the cloud-top, over-cloud and sub-cloud layers are presented for both cloud thickness groupings for each season. In the top data row, the relative frequency of cases in a group exhibiting a minimum in dry static stability in the cloud-top layer relative to the other two layers is given. The second and third data rows correspond to increasing and decreasing stability with height through the three layers, respectively. The fourth row corresponds to maximum stability in the cloud-top layer relative to the other two layers. In the last two rows, the relative frequency of cases where the over-cloud layer is more stable than the cloud-top layer and where the sub-cloud layer is more stable than the cloud-top layer are presented for each group. Simple inspection of the entries reveals that based upon this analysis any possible stratification may be observed for any given group. However, some stratifications are substantially more common than others.

### 3.1.b.i. Thick Cloud Cases

For the thick cloud cases, the most likely stratification is that with decreasing stability with height through the three layers. The relative frequency of occurrence of this structure is nearly constant with respect to season. This is also true of the structure with increasing stability with height, which is the least likely. Minimum stability in the cloud-top layer tends to be the second most likely structure, and is most common in fall and winter. Maximum stability in the cloud-top layer has the opposite seasonal variation. In spring and summer, these two stratifications are nearly equally likely to occur. In order to properly interpret each structure physically, the

corresponding values of  $\overline{\sigma_T}$ ,  $\overline{\sigma_0}$ , and  $\overline{\sigma_S}$  must be considered together with the relative frequency of occurrence of the two layer stratifications shown in the last two data rows in Table 2.

In an average season, the value of  $\sigma_0$  is greater than  $\sigma_T$  in only 42% of the thick cloud cases, however,  $\overline{\sigma_0}$  minus  $\overline{\sigma_T}$  is positive and equal to  $\sim 0.6^\circ\text{K/km}$ . This implies that, for cases where  $\sigma_0 > \sigma_T$ , the difference  $(\overline{\sigma_0} - \overline{\sigma_T})$  is larger than the difference  $(\overline{\sigma_T} - \overline{\sigma_0})$ , for cases where  $\sigma_T > \sigma_0$ . The situation of a small decrease in dry static stability from the cloud-top layer to the over-cloud layer strongly suggests that both layers are located in the same air mass. This applies to cases when the observed structures are those with either maximum stability in the cloud-top layer or decreasing stability with height through the three layers. If an expected decrease is computed for these cases, which is based upon an assumption that mean conditions are representative of those in a uniform air mass, then an estimate of a typical value of  $(\overline{\sigma_0} - \overline{\sigma_T})$  may be made for the cases when  $\sigma_0 > \sigma_T$ . This value is  $\sim 1.4^\circ \text{ K/km}$ . Thus, in the thick cloud cases where  $\sigma_0 > \sigma_T$ , the over-cloud layer tends to be stable and caps the cloud layer. This relatively stable layer may possibly be interpreted as an elevated frontal zone, since the stability of a frontal zone at this level is not nearly as great as at lower levels due to the cumulative effect of diffusion over its lifetime. However, other interpretations are possible and are considered below.

In an average season, the value of  $\sigma_S$  is greater than  $\sigma_T$  in 65% of the thick cloud cases and  $\overline{\sigma_S} - \overline{\sigma_T}$  equals  $\sim 1.75^\circ \text{ K/km}$ , which is substantial. The implication is that for cases where  $\overline{\sigma_T} > \overline{\sigma_S}$ , the difference  $(\overline{\sigma_T} - \overline{\sigma_S})$  is relatively small and that for cases where  $\overline{\sigma_S} > \overline{\sigma_T}$ ,

the difference  $(\overline{\sigma_S} - \overline{\sigma_T})$  is large. In the manner used above,  $(\overline{\sigma_S} - \overline{\sigma_T})$  is estimated to be  $\sim 2.4^\circ$  K/km, for cases where  $\overline{\sigma_S} > \overline{\sigma_T}$ . Thus, the structure with decreasing stability with height through the three layers corresponds very well to the classical notion of a very stable layer or front below the cloud layer and where the cloud-top layer and over-cloud layer exist in the same lifted air mass. This is observed to be the most likely structure for the thick cloud cases. The interpretation of the structure with minimum stability in the cloud-top layer is similar to the classical notion, except for the relatively stable capping layer.

In addition to the interpretation that the stable over-cloud layer is another frontal zone, which might exist in the case of thick clouds to be west of the center of a mature or occluded cyclone, a second interpretation is that the enhanced stability of this layer is due to both strong infrared radiative cooling and evaporative cooling in the region of cloud-top, which are greatest near the lower boundary of the over-cloud layer and, thus, tend to stabilize the over-cloud layer. Nighttime cases would show these effects more than daytime cases due to the compensating effect of solar absorption.

Observations reported by Griffith et al, 1979, of the radiative characteristics of tropical cirrus clouds lead to the conclusion that the lapse rate of a 25 mb thick over-cloud layer, as defined here, may be potentially stabilized at a rate of up to  $\sim 20^\circ$  K/km/day due to infrared radiative processes. These results correspond to the case of a high, very cold cloud (i.e.  $\sim -50^\circ$  C), which is essentially a black body with respect to infrared radiation and represents the situation of maximum radiative effect. The potential stabilization of the overcloud layer due to evaporative

processes may be evaluated by noting that typical ice water contents may range from 0.001 to 0.3 g/m and typical mean vertical velocities in the cloud layer may range from 1 to 100 cm/s (from Griffith et al, 1979, and Heymsfield, 1977). If the cloud-top level is assumed to remain constant and the ice crystals are assumed to be transported upward at the observed vertical velocity and are sublimated at cloud-top, the lapse rate of the over-cloud layer may be potentially stabilized at a rate of from  $\sim 0.005$  to  $\sim 150^\circ\text{K}/\text{km}/\text{day}$ . A vertical velocity of 2 cm/s and an ice water content of  $0.1 \text{ g}/\text{m}^3$  result in a lapse rate stabilization rate of  $\sim 10^\circ\text{K}/\text{km}/\text{day}$  in the over-cloud layer due to evaporative cooling.

Subsidence and its associated adiabatic warming may also lead to increased stability in a layer. However, in the case of a relatively stable layer directly above a relatively unstable layer, a very strong or enduring subsidence field would be required in the upper layer to explain the observed magnitude of the stability differences if both layers are initially assumed to be similar. For example, a vertical velocity of  $\sim -2 \text{ cm}/\text{s}$  results in the lapse rate being stabilized at a rate of  $\sim 0.3^\circ\text{K}/\text{km}/\text{day}$  at these levels. Large vertical gradients of both the vertical motion field and the divergence would also be required near the interface between the two layers for the observed structure to evolve by this mechanism. Such gradients may exist across elevated fronts but the vertical circulations required are opposite to those corresponding to the classical model. Compensating subsidence in the region of strong convection may affect the stability structure of middle and upper tropospheric outflow layers. However, the required vertical gradients in the circulation are not likely to be due to the



convection but rather due to some pre-existing structure. Thus, radiative and evaporative effects may readily account for the observed stability of the over-cloud layer, while adiabatic effects due to vertical motion are much less likely to be the source of the observed structure.

The structure with increasing stability with height does not correspond to the classical structure. However, if the location of cloud-top pressure is slightly in error in these cases, i. e. above the actual cloud-top level, then the stability of the cloud-top layer is overestimated since the over-cloud layer tends to be much more stable. Since, where  $\sigma_T > \sigma_S$ , the difference in stability between the cloud-top layer and the sub-cloud layer tends to be relatively small, it may be hypothesized that they are in the same air mass and that the sign of the difference, which is inconsistent with this hypothesis, arises from slight errors in the location of the cloud-top level. In any event, these cases do not appear to be forced by frontal lifting from directly below the cloud layer.

The above arguments, also, lead to the conclusion that, in the case of the structure with maximum stability in the cloud-top layer, the differences in dry static stability between the three layers tend to be relatively small. Thus, the presence of a very stable layer is not indicated for any of the layers. The observations of maximum stability in the cloud-top layer may be due to the effects of infrared radiation or evaporation near cloud-top coupled with a slight mislocation of the cloud-top level. In this instance, maximum stability occurs just above cloud-top. It should be noted; that the interpretations, which rely on assumed errors in the location of cloud-top, lead to the conclusion that  $\overline{\sigma_T}$  has been overestimated.

Combining all the results from the analysis of the stratification about thick clouds, the following conclusions may be put forth:

1. In 65% of the cases, the mean sub-cloud layer is estimated to be  $\sim 2^\circ\text{K}/\text{km}$  more stable than mean conditions. This strongly suggests the presence of a frontal zone corresponding to the classical model.
2. In nearly half of the cases with the stable sub- cloud layer, the mean over-cloud layer is also relatively stable, i.e. estimated to be  $\sim 1.3^\circ\text{K}/\text{km}$  more stable than mean conditions.
3. In  $\sim 35\%$  of the cases, which do not show the stable sub-cloud layer,  $\sim \frac{1}{3}$  do exhibit the stable capping layer, while the rest show a weak tendency for maximum stability in the vicinity of cloud-top.
4. The stability of the mean cloud-top layer has probably been slightly overestimated due to the mislocation of the cloud-top level in some cases. However, even if  $\overline{\sigma_T}$  is adjusted to compensate for this effect, the corresponding temperature lapse rate is still 1 to  $2^\circ\text{K}/\text{km}$  less than the moist adiabatic lapse rate. It is primarily the moisture content of this layer, which distinguishes it from mean atmospheric conditions.

These conclusions were based on an average season. They are most valid in winter, where the magnitude of the differences are larger than for the average season.

### 3.1.b.ii. Thin Cloud Cases

For the thin cloud cases, tin- structure with minimum stability in the cloud-top layer is the most likely stratification in each season. However,

maximum stability in this layer is the next most commonly observed structure. Increasing stability with height through the three layers is slightly more common than decreasing stability with height. The observed relative frequency of occurrence for each structure for the thin cloud cases exhibits a seasonal range of  $\sim 5\%$ . No obvious pattern is evident in this seasonal variation. The observed relative frequency of occurrence for the different stratifications indicates substantial differences between the thick and thin cloud cases.

In an average season, the value of  $\sigma_0$  is greater than  $\sigma_T$  in  $\sim 60\%$  of the thin cloud cases and the difference  $(\overline{\sigma_0} - \overline{\sigma_T})$  is  $\sim 2.2^\circ$  K/km. This difference is very large considering the proximity of these two layers and the above percentage. If for the cases where  $\sigma_0 < \sigma_T$ , the overcloud layer and the cloud-top layer are assumed to exist in the same air mass and an expected value of  $(\overline{\sigma_T} - \overline{\sigma_0})$  is computed based on mean conditions, then an estimate can be made for  $(\overline{\sigma_0} - \overline{\sigma_T})$  for the cases when  $\sigma_T < \sigma_0$ . This estimate is that  $(\overline{\sigma_0} - \overline{\sigma_T})$  equals  $\sim 3.7^\circ$  K/km. This indicates a very stable capping layer for the cases when  $\sigma_0 > \sigma_T$ . This conclusion relies on the above estimate only in degree and not in substance. The stability of the over-cloud layer when  $\sigma_0 > \sigma_T$  is much greater for the thin cloud cases when compared to the corresponding thick cloud cases. Whereas the interpretation that these cases represent cloud layers capped by a frontal zone is somewhat open to question, as noted previously for the thick cloud cases; it is much more plausible here, given the estimated magnitude of  $\overline{\sigma_0}$  for the thin cloud cases. The estimated value of  $\overline{\sigma_0} \cong 7^\circ$  K/km for the thin cloud cases where  $\sigma_0 > \sigma_T$ , corresponds to a temperature lapse rate of only  $\sim 4.5^\circ$  K/km. Radiative

and evaporative processes may be responsible for the evolution of this structure.

In an average season, the value of  $\sigma_S$  is greater than  $\sigma_T$  in 57% of the cases. The difference  $\overline{\sigma_T} - \overline{\sigma_S}$  is relatively small and equal to  $\sim 0.2^\circ\text{K/km}$ . This difference is expected to be  $\sim -0.1^\circ\text{K/km}$  if both layers exist in the same air mass. If this is correct for the thin cloud cases, where  $\sigma_T < \sigma_S$ ; then for the cases where  $\sigma_S < \sigma_T$ , the difference may be estimated to be  $\sim 0.6^\circ\text{K/km}$ . This implies that, for the structures exhibiting either maximum stability in the cloud-top layer or increasing stability with height, the cloud-top layer is somewhat more stable than the sub-cloud layer but not so stable as to suggest a frontal zone.

In light of the above arguments, the observed stratifications for the thin cloud cases may be interpreted in an average sense for a mean season. The structure with decreasing stability with height through the three layers appears to be associated with the situation of all three layers existing in the same air mass. There is no indication of a frontal zone in the sub-cloud layer for this structure as there is for the thick cloud cases. Also, where this structure was the most frequently observed stratification for the thick cloud cases, it is the least frequently observed for the thin cloud cases. The stratification where minimum stability is observed in the cloud-top layer of thin clouds corresponds to the situation where the cloud layer and sub-cloud layer are located in the same air mass. A very stable layer is observed in the over-cloud layer and no indication of a frontal zone is found for the sub-cloud layer. The structure with increasing stability with height, also, shows the very stable over-cloud layer and no sub-cloud front. The

enhanced stability of the cloud-top layer, i.e.  $0.6^\circ\text{K/km}$  greater than  $\sigma_s$  is most likely due to small errors in the location of the cloud-top level. This interpretation seems reasonable given the very stable nature of the over-cloud layer. This interpretation leads to the conclusion that  $\overline{\sigma_T}$  has been overestimated. For the structure with maximum stability in the cloud-top layer, the cloud-top layer and over-cloud layer appear to be located in the same air mass due to the small decrease with height of dry static stability for the layers. However, the stability of the cloud-top layer is not sufficiently great to warrant an interpretation based on the presence of a frontal zone. It is possible that errors in the location of the cloud top level together with radiative and evaporative effects lead to the observed maximum. In any event, this stratification is very similar to the decreasing stability with height structure except for the weak maximum, i.e. none of the three layers exhibit sufficient stability for a frontal zone.

Combining the above results, the conclusions from the analysis of the stratification about thin cloud layers may be summarized as:

1. In  $\sim 60\%$  of the cases, a very stable mean over-cloud layer exists, whose stability strongly suggests the presence of a front, i.e.  $\sigma_0 \sim 7^\circ\text{K/km}$ .
2. In the other 40% of the cases, the presence of a frontal zone or a very stable layer is not indicated for any of the three mean layers. However, in 60% of these cases there is an indication of enhanced stability in the vicinity of mean cloud-top level.
3. It is likely that, when maximum stability is observed to increase with height through the three layers, the location of

cloud-top is slightly in error. If this is true, then  $\overline{\sigma_T}$  has been overestimated. If the magnitude of this error is estimated from mean conditions, then a corrected value of  $\overline{\sigma_T}$  may be computed, which is slightly less than  $\overline{\sigma_S}$ .

The above inferences for the thin cloud cases are nearly equally valid for any season. The conclusions for both the thin and thick cloud cases are based upon observed means and the relative frequency of occurrence of various structures. It must be emphasized that they only apply to the average case exhibiting such a structure.

### 3.1.c. Relative Frequency Distributions of Stability

As was stated previously, any possible stability stratification may be observed for these three layers for a cloud case. In fact, the observed stability values range over a wide domain. Conditions ranging from super-adiabatic to strong inversions are observed in each of the three layers in each season. Errors in the location of cloud-top pressure have been assumed to account for some of the observations of stable cloud-top layers. At this point, it is appropriate to examine the observed distribution of dry static stability for each layer.

In Figure 6, the observed relative frequency of occurrence is given for various stability classes. In each panel, the distributions are given for each season for one of the three layers for a particular cloud thickness group. Each class represents a  $1^\circ\text{K}/\text{km}$  range of observed dry static stability, except for class 1. Cases included in class 1 correspond to observations of super adiabatic or dry adiabatic

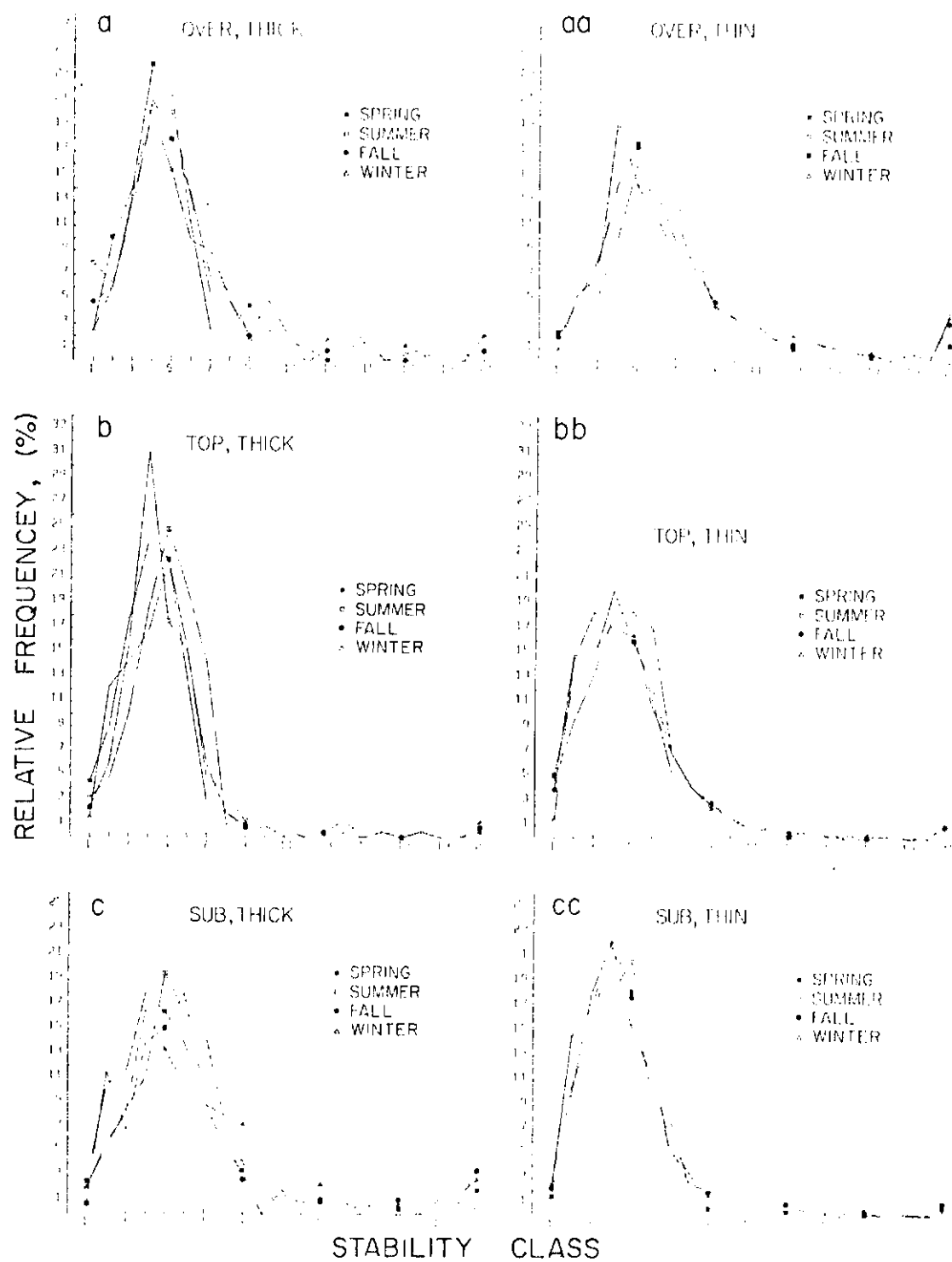


Figure 6. Relative frequency of occurrence of various stability classes for each season for the thick cloud cases for each layer, (i.e. (a) over-cloud layer, (b) cloud-top layer, (c) sub-cloud layer) and, similarly, for the thin cloud cases (i.e. (aa), (bb) and (cc), respectively). See text for definition of stability classes and further explanation.

conditions, i.e.  $\sigma \leq 0^\circ\text{K/km}$ . Class number 2 includes observations where  $0^\circ\text{K/km} < \sigma < 1^\circ\text{K/km}$ . Similarly, class N includes cases where  $(N-2)^\circ\text{K/km} < \sigma < (N-1)^\circ\text{K/km}$ . Note that class 2 represents cases, where conditions are approximately moist adiabatic for the pressure and temperature domain of these cloud cases. Some of the cases included in class 3 may also correspond to moist adiabatic conditions. In general for this domain, class 14 corresponds to near isothermal conditions in a layer, though some cases in classes 13 and 15 may also show this due to their respective pressure levels. Classes 16 through 21 correspond to cases exhibiting an inversion in the layer with the strength of the observed inversion increasing with class number, e.g. class 21 includes cases where temperature typically increases at a rate of greater than  $\sim 5^\circ \text{ K/km}$  from the base to the top of the layer. In order to facilitate the consideration of these data, the corresponding cumulative frequency distributions are given in Figures 7 and 8 for the thick cloud cases and for the thin cloud cases, respectively. The relative frequencies are accumulated progressively from class 1 through class 21, e.g. the cumulative frequency plotted for class 3 corresponds to the sum of the relative frequencies of classes 1, 2 and 3. In each panel, the observed distributions for each of the layers are given for a particular season and cloud thickness group.

In general, the relative frequency distributions are broader for the thin cloud cases in the over-cloud layer and the cloud-top layer, when compared to the thick cloud cases. The opposite is true of the sub-cloud layer. Narrow distributions correspond to uniform conditions observed on a case by case basis. In winter, the distributions tend to be broader than in other seasons. There is also a tendency for a seasonal shift in the distributions, i.e. the summer peak is generally to



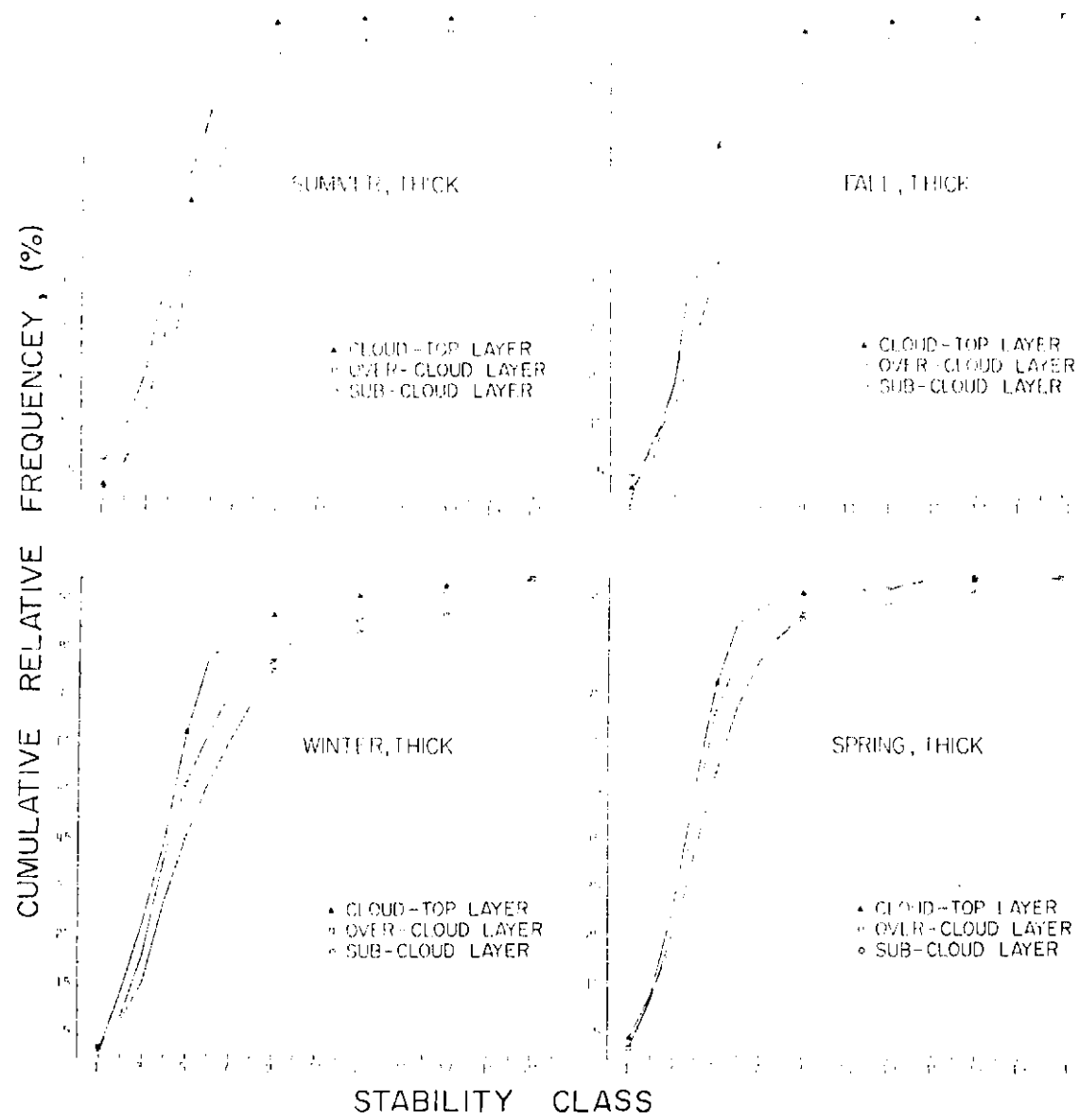


Figure 7. Cumulative relative frequency distributions of stability class for the thick cloud cases for each of the over-cloud, cloud-top and sub-cloud layers. See text for further explanation.

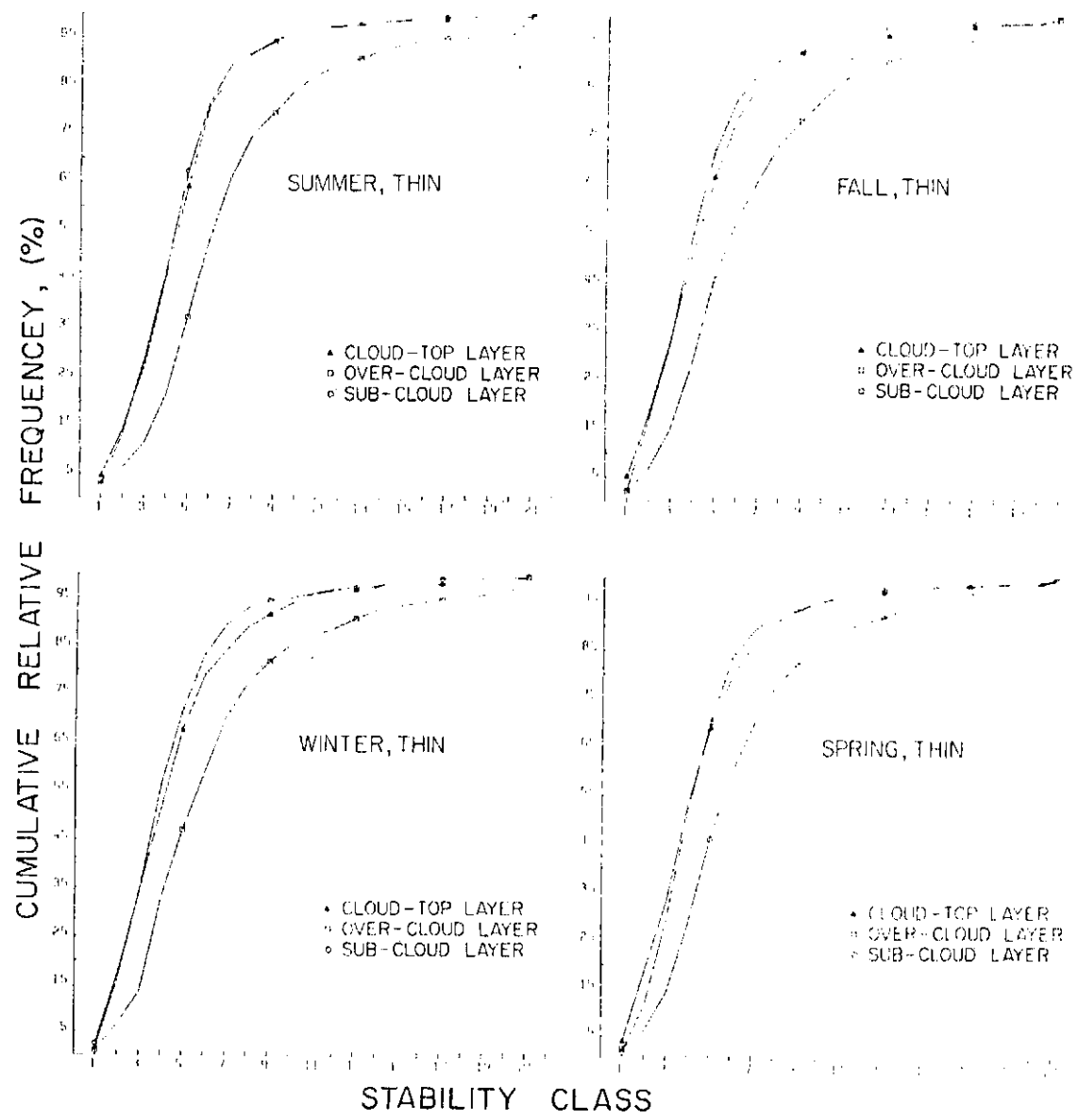


Figure 8. Same as for Figure 7, except for thin cloud cases.

the right and the winter peak tends to be to the left of the peaks for spring and fall. It should also be noted that the over-cloud layer distributions show a relatively large frequency of very stable conditions, especially for the thin cloud cases. The sub-cloud layer distributions for the thick cloud cases, also, exhibit a relatively large frequency of very stable conditions.

The median values of  $\sigma_o$ ,  $\sigma_T$ , and  $\sigma_S$  (i.e. cumulative frequency = 50%, see Figs. 7 and 8) exhibit the same relative pattern as the mean values depicted in Figure 5, except for thick cloud cases in summer. However, the differences between the median values of  $\sigma_o$ ,  $\sigma_T$ , and  $\sigma_S$  for a given season are smaller than noted for the means. Thus, the relative frequency of very stable conditions for the various layers has a substantial influence on the computed means. The median values of  $\sigma_T$  and  $\sigma_S$  for the thin cloud cases are within 1 to 2°K/km of the stability associated with moist adiabatic conditions, while the median values of  $\sigma_o$  are an additional 1.5°K/km more stable. For the thick cloud cases, the median values of  $\sigma_T$  and  $\sigma_o$  are within 1 to 2°K/km of moist adiabatic conditions, while the median value of  $\sigma_S$  is an additional 1°K/km more stable. Note that dry adiabatic or super adiabatic conditions tend to be most common in the over-cloud layer for the thick cloud cases and in the cloud-top layer for the thin cloud cases, when compared to the other layers.

For the thin cloud cases, the cumulative relative frequency distributions for the sub-cloud layer and the cloud-top layer are very similar. There is a slight tendency for the cloud-top layer to exhibit more extreme values, when compared to the sub-cloud layer. Fewer than 5% of the observations of  $\sigma_T$  or  $\sigma_S$  indicate isothermal or inversion conditions. The

distributions for  $\sigma_0$  are substantially different. Approximately 10% of the observations of  $\sigma_0$  correspond to isothermal or inversion conditions. Moderately stable to very stable conditions dominate the  $\sigma_0$  distributions. The  $\sigma_0$  distributions for the thin cloud cases are the most stable of all the layers for either thickness group.

Noting the distributions for the thick cloud cases, in no season do two layers exhibit the degree of similarity seen between the cloud-top and sub-cloud layers for the thin cloud cases. Also, no two layers are as different as the over-cloud and cloud-top layers for the thin cloud cases. The seasonal variation in the distributions is greater than for the thin cloud cases. In summer, the over-cloud layer and the sub-cloud layer exhibit very stable conditions in nearly the same percentage of cases, while in the other seasons the sub-cloud layer is approximately twice as likely to show this. As in the thin cloud distributions, the cloud-top layer exhibits very stable conditions, i.e. isothermal, less than ~5% of the time.

### 3.2 Vertical Wind Shear

The results of the analyses of the vertical shear of the horizontal wind speed in the cloud-top layer,  $S_t$  the over-cloud layer,  $S_o$ ; and the sub-cloud layer,  $S_s$ , are presented in this section. Recall that the wind direction is ignored in these analyses.

Considering the sign of the shear, it is apparent that negative shear occurs relatively infrequently in these layers. For the thin cloud cases in a given season, the relative frequency of occurrence of negative shear is nearly the same for each layer. Seasonal variation is also negligible, except for the summer season, where

approximately 20% of the cases exhibit negative shear in a given layer compared to 15 to 16% in the other seasons. The thick cloud cases have both a more pronounced seasonal variation and more significant differences between the layers in a given season, than the thin cloud cases. For the thick cloud cases,  $S_T$ ;  $S_0$  and  $S_s$  are negative in 11, 11 and 14% of the winter cases; in 13, 15 and 18% of the fall cases; in 17, 19 and 26% of the spring cases; and in 17, 24 and 29% of the summer cases, respectively. Thus, as in the thin cloud cases, negative shear occurs most frequently in the summer for each layer. Negative shear is least likely in winter and the cloud-top layer is the layer least likely to exhibit negative shear in each season for the thick cloud cases. However, the difference between this layer and the over-cloud layer is relatively small except in summer. Differences between the cloud-top layer and the sub-cloud layer are larger and are most pronounced in spring and summer. Thus, for a given cloud thickness group in a given season, the relative frequency of negative shear does not vary substantially among layers in close proximity, i.e. all three layers of the thin cloud cases or the upper two layers for the thick cloud cases.

In terms of the relative frequency of occurrence of negative shear in the three layers for the thick cloud cases, spring is more similar to summer than to fall and fall is more similar to winter than to spring. The seasonal variation for the thick cloud cases may be at least partly explained by noting that the thick cloud is likely to occur in a region of strong or deep vertical lifting in the middle and upper levels, i.e. in association with either an elevated warm front or to a lesser degree an elevated cold front of a cyclone. This is particularly true in the cold seasons. This region is located near

the fastest upper level flow associated with the cyclone, i. e. the jet stream core, whose strength is coupled to the cyclone intensity. The intensification of the flow, particularly at high levels, over the region of strong uplift makes positive shear more likely in layers below the jet stream level and above the front. Thus, the seasonal cycle in cyclone intensity and the associated upper level flow may produce the observed seasonal variation in the relative frequency of negative shear for thick cloud layers. Since the thin cloud is likely to occur in a region of weak vertical lifting, seasonal changes in cyclone intensity are more likely to affect the areal extent than the shear environment of the thin clouds. This is because even though a more intense cyclone has a stronger jet core and a larger area of faster flow, the region of strong uplift is larger and, thus, the weak uplift region is located farther away from the jet core compared to the less intense cyclone case.

Another factor, which might influence the seasonal cycle, is the role of vertical transport of water by deep convection in the formation of some of these clouds. Deep convection is most common in summer and spring, less common in fall and rare in winter for this domain. Thus, the seasonal cycle of deep convection resembles the seasonal variation in the relative frequency of negative shear for the thick cloud cases. Deep convection tends to occur in close proximity to a cold front at the surface and the associated upper level jet stream, particularly in spring. This region is generally upstream from the jet maximum and is not in an area of strong middle or upper level large-scale lifting. Horizontal propagation of the convection away

from the surface front or horizontal transport of water after injection into the middle and upper levels may cause the outflow cloud layer to exist away from under the jet core. Thus, if deep convection is important in the formation of some of these thick cloud cases, then these cases may exist in a substantially different environment in terms of large-scale vertical motion and the strength of the upper level flow compared to cases associated with elevated fronts, which are typical of the winter season.

There are eight possible configurations for the sign of the shear in the three layers of a given cloud case. In Table 3, the observed relative frequency of occurrence for each of these configurations is given for each season for the thick cloud cases, (a), and for the thin cloud cases, (b). The predominance of positive shear may be further emphasized by noting that positive shear of the horizontal wind speed is observed in two or more of the three layers in 84% to 94% of the thick cloud cases and in 86% to 92% of the thin cloud cases depending on the season. Positive shear in all three layers is the most common configuration in every season for either cloud thickness group. Nearly one-half to greater than two-thirds of the cases exhibit this structure in a given season for either group. The next most likely configurations are those involving negative shear in only one of the layers. For the thin cloud cases, none of these three structures is significantly more likely than any other, except in summer. In fact, the spring, winter and fall seasons show almost no seasonal variability in the relative frequency of any given configuration. This lack of seasonal variability in the occurrence of the different configurations corresponds exactly to the result noted above, from the analysis of

(a)

## Thick Cloud Cases

$S_0$	$S_T$	$S_s$	Su	F	W	Sp	Average	Range
+	+	+	47	63	70	51	58	23
+	+	-	19	14	11	16	15	7
-	+	+	9	7	6	12	9	6
-	+	-	8	2	1	4	4	7
+	-	+	9	6	7	8	7	3
+	-	-	1	2	1	5	2	4
-	-	+	6	5	3	4	4	3
-	-	-	1	1	1	0	1	1

(b)

## Thin Cloud Cases

			Su	F	W	Sp	Average	Range
+	+	+	56	65	65	66	63	9
+	+	-	13	9	9	7	10	5
-	+	+	10	10	8	10	10	2
-	+	-	2	1	2	1	2	1
+	-	+	7	8	7	8	7	1
+	-	-	5	3	4	2	3	3
-	-	+	5	3	4	4	4	2
-	-	-	2	1	1	2	1	1

Table 3. Relative frequency of occurrence in percent of cases having various configurations for the sign of the vertical shear of the horizontal wind speed in the over-cloud, cloud-top and sub-cloud layers, i.e. sign of  $S_0$ ,  $S_T$  and  $S_s$ , respectively, for each season (a) for thick cloud cases and (b) for thin cloud cases. Values for the average season and the seasonal range are also given for each configuration.



the sign of the shear in each layer independently. In summer, the configuration with negative shear in only the sub-cloud layer is somewhat more likely than in other seasons and the configurations with negative shear in at least two layers tend to be slightly more common. The relative frequency of occurrence for the other two structures with positive shear in only two of the layers does not change significantly even in summer, i.e. only the structure with all positive shear is less likely in summer.

For the thick cloud cases, the seasonal range of relative frequency for each configuration is larger than for the thin cloud cases. In general, the spring/fall season values are most similar to the summer/winter values. These results are the same as those derived from the analysis of each layer independently. Other than the seasonal variation, the primary difference between the thick and thin cloud cases is that the structure with negative shear in only the sub-cloud layer is substantially more likely for the thick cloud cases in all seasons. Considering the average of the seasonal values, the increased frequency of this structure is almost equal to the decreased frequency of the structure with all positive shear compared to the thin cloud cases. This is not true on a season by season basis, where the relative frequency of occurrence for the other structures with at least one positive shear layer and negative shear in the sub-cloud layer are also somewhat different, when comparing the thin and thick cloud cases.

For the analysis of the magnitude of the vertical shear of the horizontal wind speed in each of the three layers, cases exhibiting positive shear and cases exhibiting negative shear in the layer of

interest are considered independently. The following discussion is limited to seasonal means. As in the case of the dry static stability, the means encompass quite a wide range of observed values. The standard deviations for the various means typically range from nearly equal to the mean to approximately twice the mean value. In Table 4, the average shear in each layer for each season is given for cases with positive shear in the layer,  $\overline{S}_+$ , and for cases with negative shear in the layer,  $\overline{S}_-$ , for the thick cloud cases (a) and for the thin cloud cases (b). The values of  $\overline{S}_+$  and  $\overline{S}_-$  may be combined with the corresponding observed relative frequency of occurrence given above to obtain either  $\overline{S}$  or  $|\overline{S}|$ , i. e. the seasonal mean shear or the seasonal mean magnitude of the shear, respectively.

Considering  $\overline{S}_+$ , both the thick cloud and thin cloud cases show a maximum in winter, a minimum in summer, and spring values larger than fall values for each layer. The seasonal pattern for  $\overline{S}_-$  is somewhat more confused. Due to the small relative frequency of negative shear, the pattern for  $|\overline{S}|$  resembles that for  $\overline{S}_+$  very closely. The seasonal range of  $\overline{S}_-$  is generally less than one-half that of  $\overline{S}_+$  for each layer for either thickness group. Thus, the seasonal cycle in cyclone intensity and speed of the upper level flow affects the positive shear cases much more than the negative shear cases. As in the case of the sign of the shear, the thick cloud cases have a substantially greater seasonal range in both  $\overline{S}_+$  and  $\overline{S}_-$  for a given layer, when compared to the thin cloud cases. This supports the earlier conclusion based on the analysis of the sign of the shear, that the thin cloud cases are not as sensitive as the thick cloud cases to the seasonal cycle in cyclone intensity. In general,  $\overline{S}_+$  is greater and  $|\overline{S}_-|$  is less for the

(a)				
Thick Cloud Cases				
	Su	F	W	Sp
0	4.0	4.9	6.5	6.1
	-4.5	-4.9	-5.5	-4.6
T	3.3	4.8	6.5	5.5
	-3.8	-4.5	-5.4	-4.6
S	4.1	5.1	6.8	5.5
	-5.7	-5.0	-5.5	-4.4

(b)				
Thin Cloud Cases				
	Su	F	W	Sp
0	4.1	4.7	6.0	4.9
	-5.3	-5.4	-4.9	-5.2
T	3.8	4.6	5.4	5.2
	-5.0	-5.4	-5.9	-5.9
S	3.4	4.7	5.4	5.1
	-5.3	-5.4	-5.4	-4.7

Table 4. Mean vertical shear of the horizontal wind speed in m/s/km for each season (a) for thick cloud cases and (b) for thin cloud cases for the over-cloud, cloud-top, and sub-cloud layers, i.e. 0, T and S, respectively. The positive entries are the means for cases with positive shear in that layer, i.e.  $\overline{S_+}$ , and the negative entries are the means for cases with negative shear in that layer, i.e.  $\overline{S_-}$ .

thick cloud cases, when compared to the thin cloud cases for a given season and layer. For the thin cloud cases,  $\overline{|\mathbf{S}_-|} > \overline{\mathbf{S}_+}$  in most instances, while except in summer,  $\overline{\mathbf{S}_+} > \overline{|\mathbf{S}_-|}$  for the thick cloud cases. Thus, in the mean for a season, when negative shear occurs in one of the layers of a thin cloud, the magnitude of the shear tends to be greater than when positive shear occurs in that layer. This is a surprising result.

For the thick cloud cases, the minimum values of  $\overline{\mathbf{S}_+}$ ,  $\overline{|\mathbf{S}_-|}$ , and  $\overline{|\mathbf{S}|}$  occur in the cloud-top layer for each season except in spring, where the minimum values of  $\overline{|\mathbf{S}_-|}$  and  $\overline{|\mathbf{S}|}$  occur in the sub-cloud layer. The maximum values occur in the sub-cloud layer in each season except spring, where the maximum values of  $\overline{|\mathbf{S}_-|}$  and  $\overline{|\mathbf{S}|}$  occur in the cloud-top layer. For the thin cloud cases, the maximum values of  $\overline{\mathbf{S}_+}$  and  $\overline{|\mathbf{S}|}$  occur in the over-cloud layer in each season except spring, where the maximum values occur in the cloud-top layer. The maximum value of  $\overline{|\mathbf{S}_-|}$  occurs in the cloud-top layer in each season except summer, where it occurs in the sub-cloud layer. The pattern for minimum values of  $\overline{\mathbf{S}_+}$ ,  $\overline{|\mathbf{S}_-|}$ , and  $\overline{|\mathbf{S}|}$  is confused. Except in winter, the difference between the maximum and minimum values of either  $\overline{\mathbf{S}_+}$ ,  $\overline{|\mathbf{S}_-|}$ , and  $\overline{|\mathbf{S}|}$  observed for the three layers in a season is larger for the thick cloud cases than for the thin cloud cases. Thus, more variability between the layers is observed for the thick cloud cases than for the thin cloud cases, except in winter.

On a case-by-case basis, four possible structures for the magnitude of the shear may occur. These are: maximum  $|\mathbf{S}|$  in the cloud-top layer, decreasing  $|\mathbf{S}|$  with height through the three layers, increasing  $|\mathbf{S}|$  with height, and minimum  $|\mathbf{S}|$  in the cloud-top layer. In Table 5,

(a)

Thick Cloud Cases

	Su	F	W	Sp	Average	Range
$ S_T  \geq  S_0 $ and $ S_s $	32	33	31	28	31	5
$ S_s  >  S_T  \geq  S_0 $	18	22	20	22	20	4
$ S_0  >  S_T  \geq  S_s $	16	19	23	17	19	7
$ S_T  <  S_0 $ and $ S_s $	34	26	26	33	30	8

(b)

Thin Cloud Cases

	Su	F	W	Sp	Average	Range
$ S_T  \geq  S_0 $ and $ S_s $	34	34	33	37	34	4
$ S_s  >  S_T  >  S_0 $	20	22	21	22	21	2
$ S_0  >  S_T  \geq  S_s $	20	20	21	22	21	2
$ S_T  <  S_0 $ and $ S_s $	26	24	25	19	24	7

Table 5. Relative frequency of occurrence in percent of cases having various relative configurations of the magnitude of the vertical shear of the horizontal wind speed in the over-cloud, cloud-top and sub-cloud layers, i.e.  $|S_0|$ ,  $|S_T|$  and  $|S_s|$ , respectively, for each season. Values for the average season and the seasonal range are also given for each configuration.

the observed relative frequency of occurrence of each of these structures for each season for both the thick cloud cases (a) and the thin cloud cases (b) is given.

The seasonal variability of the relative frequency of occurrence of each structure is larger for the thick cloud cases than for the thin cloud cases. The two most commonly observed structures for the thick cloud cases in each season are those with either maximum or minimum shear magnitude in the cloud-top layer. On an annual basis, they are  $\sim 50\%$  more likely than the other two structures. In spring, the structure with maximum  $|S|$  in the cloud-top layer is somewhat less likely than in the other seasons. The structure with minimum shear in the cloud-top layer is substantially less likely in fall and winter when compared to spring and summer, where it is the most commonly observed structure. This structure corresponds to the mean structure for each season, noted above, which was derived from the analysis of each layer independently. Thus, in fall and winter, the most likely structure does not correspond to the observed mean structure. If the cases of increasing or decreasing  $|S|$  with height can be assumed to cancel in the computation of the mean structure, this implies that if a typical case with minimum  $|S|$  in the cloud-top layer is compared to a typical case with a maximum  $|S|$  in the cloud-top layer, the minimum would be more pronounced than the maximum.

For the thin cloud cases, the structure with maximum  $|S|$  in the cloud-top layer is the most likely structure in each season. The observed relative frequency of occurrence for each structure is nearly constant with respect to season except in spring where the structure with minimum  $|S|$  in

the cloud-top layer is less likely and the structure with maximum  $|S|$  in the cloud-top layer is more likely than in the other seasons. This is opposite to what is observed in the thick cloud cases. Except in spring, the most likely structure for the thin cloud cases does not correspond to the mean structure for a season, given in Table 4b.

### 3.3 Richardson Number

The results of the analyses of the Richardson number in the over-cloud, cloud-top, and sub-cloud layers, i.e.  $R_0$ ,  $R_T$  and  $R_S$ , respectively, are discussed in this section. Richardson numbers for the 350 mb to 450 mb layer,  $R_4$ , and the 650 mb to 750 mb layer,  $R_7$ , are also considered.

Seasonal mean Richardson number for a layer is not a very useful quantity. This is primarily due to the inverse-square dependence of  $R$  on the vertical wind shear,  $S$ . For cases where  $S$  is small,  $R$  is very large and greatly affects the means and corresponding standard deviations. For these analyses, if  $S = 0$  or if  $R \geq 60$ , then  $R$  is arbitrarily set equal to 60. For all the layers considered, both the seasonal mean Richardson numbers and the corresponding standard deviations are largest in summer and smallest in winter. The fall and spring values are generally close to the winter values, i.e. always closer to winter than to summer. For the thick cloud cases, the values of  $\overline{R_0}$ ,  $\overline{R_T}$ , and  $\overline{R_S}$  each range from  $\sim 12$  to  $\sim 18$  with corresponding standard deviations of from  $\sim 19$  to  $\sim 31$ . For the thin cloud cases, the value of  $\overline{R_0}$  ranges from  $\sim 14$  to  $\sim 19$  with standard deviations of from  $\sim 18$  to  $\sim 24$ , respectively. The values of  $\overline{R_T}$  and  $\overline{R_S}$  each range from  $\sim 13$  to  $\sim 16$  with standard deviations from  $\sim 18$  to  $\sim 22$ , respectively. The values of  $\overline{R_4}$  and  $\overline{R_7}$ , each range from  $\sim 14$  to  $\sim 16$ . The analysis of Richardson number over thick layers, such as for  $R_4$  and  $R_7$ , is not very interesting. Less than 1% of all sondes have either

$R_i$  or  $R_r$  values within a factor of two of the turbulence threshold, i.e.  $R \leq 0.5$ . This result is unchanged if only cloud case sondes are used. The percentage of all sondes exhibiting values of  $R_r$  or  $R_i$  less than or equal to 4.0 ranges from  $\sim 10\%$  to  $\sim 30\%$  for  $R_i$  and from  $\sim 15\%$  to  $\sim 20\%$  for  $R_r$  with the minimum values occurring in summer and the maximum values occurring in winter. These values are increased by a couple of percentage points, if only cloud case sondes are used.

For the following discussion, no distinction is made between thick and thin cloud cases. Differences between these groups are considered later. In Figure 9, the relative frequency of occurrence of cloud cases with Richardson number less than or equal to a given value in each of the over-cloud, cloud-top, and sub-cloud layers is given for both the summer and winter seasons. Similar plots for fall and spring lie between the corresponding winter and summer curves and are generally closer to the winter curve. In summer, a higher percentage of the cloud cases have values of  $R_0$ ,  $R_T$  and  $R_S$  less than or equal to 0.25, when compared to the winter season. However, the winter cases show a larger relative frequency of  $R_0$ ,  $R_T$  and  $R_S$  less than or equal to 4.0, i.e. relatively small Richardson number, when compared to the summer season. In all seasons, the relative frequency of cases with Richardson number less than some given value is greatest for the cloud-top layer and smallest for the over-cloud layer. This does not hold for the smallest Richardson numbers, as in winter, the sub-cloud layer most frequently exhibits values less than  $\sim 0.2$  and in summer, the



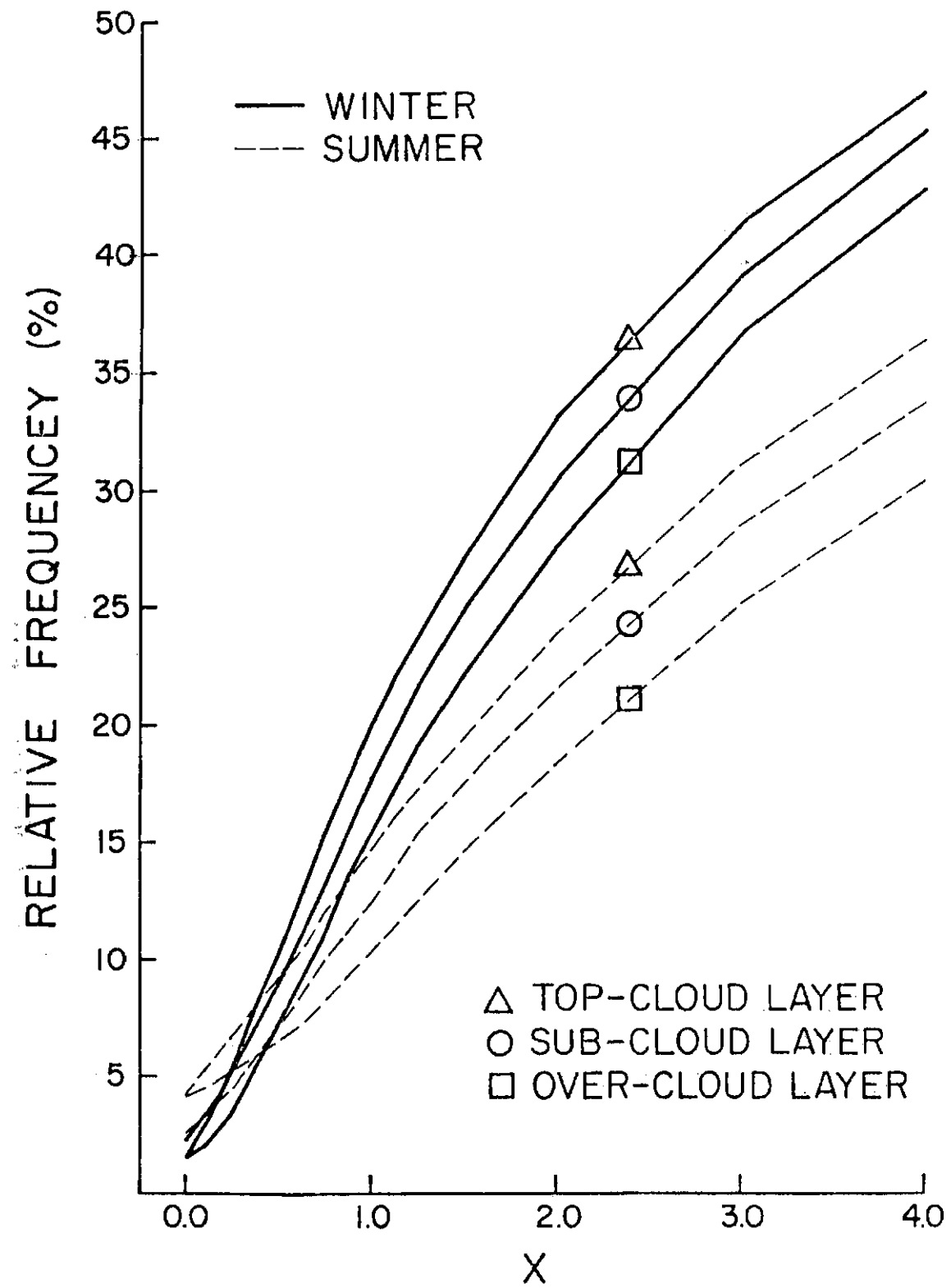


Figure 9. Relative frequency of occurrence of cloud cases having Richardson number less than or equal to  $X$  for each of the over-cloud, cloud-top and sub-cloud layers in winter and in summer.

sub-cloud layer least frequently exhibits values less than  $\sim 0.4$ . The cloud-top layer possesses the maximum Richardson number of the three layers in nearly 40% of the cases in an average season. However, in nearly 35% of the cases, minimum Richardson number is observed in this layer.

The data shown in Figure 9 and the preceding discussion are most applicable to the thin cloud cases due to the dominance of these cases in the total cloud case sample. For the thick cloud cases, the smallest values of Richardson number tend to be less common for the sub-cloud and cloud-top layers and more likely for the over-cloud layer, when compared to the thin cloud cases. The differences in relative frequency amount to less than 3% between the two groups at Richardson numbers less than 0.5 in each season. Considering cases exhibiting Richardson numbers less than or equal to 4.0, the same pattern is found though the differences between the thin and thick cloud cases for a given layer are larger, i.e.  $\sim 12\%$  maximum difference.

A Richardson number of  $\sim 0.25$  or less for the mean flow is required for turbulence and turbulent transports to be maintained by the mean flow. Since only a small percentage of these cases exhibit such small Richardson numbers, it is concluded that, in general, these clouds are not formed as a result of widespread turbulence generated by the mean flow. The Richardson number quantifies the relative importance of buoyancy forces and mechanical forces, i.e. shear, in the production of turbulent kinetic energy and, thus, also the turbulent energy transports. Considering the cloud-top layer, in only 20% of the winter cases and in only 15% of the summer cases, is the mechanical production greater than or equal to the buoyancy production. Thus, in general, buoyancy forces are the more dominant factor influencing the

production of turbulent kinetic energy and the associated convective energy transports for middle and upper tropospheric stratiform clouds. Therefore, it is primarily thermal perturbations and not wind speed perturbations that are responsible for vertical eddy circulations within these clouds.

These analyses seem to be sensitive to the vertical resolution of the data set. This may be seen by comparing the relative frequency of the very small values of Richardson number, i. e.  $\leq 0.25$ , for the cloud-top layer to that of the 350 mb to 450 mb layer for cloud case sondes. The difference in relative frequency is more than an order of magnitude. The mean cloud-top layer is  $\sim \frac{1}{3}$  the pressure thickness of the 350 mb to 450 mb layer. It is possible that with better vertical resolution, the smallest values of Richardson number may occur more frequently. However, since all significant levels are included in the rawinsonde data set, we suggest that this problem is minor.

Recall that slight errors in the location of cloud-top pressure were hypothesized based on the analysis of dry static stability, i. e. Section 3.1. If this is true, then the effect on the frequency distribution of Richardson numbers is to reduce the relative frequency of small values for the over-cloud layer and increase the relative frequency of small values for the cloud-top layer. It is unlikely that these adjustments would substantially alter the above conclusions.

#### 4. SUMMARY AND CONCLUSIONS

This study characterizes the static environment of middle and upper tropospheric stratiform clouds as deduced from rawinsonde data from 24 continental U.S. stations between 30°N and 50°N latitude for the year 1977. The analyses are limited to pressures less than 500 mb and temperatures between 0 °C and -40 °C. Thus, primarily ice-phase cloud forms are considered. Computed relative humidity with respect to ice is used to diagnose the presence of a cloud layer. Good agreement is found between climatological estimates of seasonal mean middle and upper tropospheric cloud cover deduced from surface observations and estimates based on this technique.

Thin cloud layers and thick cloud layers are treated independently. A saturated layer which is less than or equal to 50 mb thick is designated as a thin cloud case. Otherwise, the saturated layer is defined as a thick cloud case. The analyses are performed on a seasonal basis. No regional distinctions are attempted.

Three layers are defined for the analysis of a cloud case. These are the uppermost saturated layer, the next higher layer and the layer below the lowest saturated layer, i.e. the cloud-top layer, the overcloud layer and the sub-cloud layer, respectively. Cloud cases with missing data at any of the levels defining these layers are eliminated from the analyses. Over 3600 cloud cases qualified for the analysis. For each of the layers, the dry static stability, the vertical shear of the horizontal wind speed and the atmospheric analog of the Richardson number are computed. Seasonal means for each of these quantities for both cloud thickness groups are presented. The

corresponding relative frequency distributions are also presented for some of these quantities. In addition, various structures for each parameter are defined in terms of the relative values of the parameter in each of the three layers, e.g. increasing stability with height through the three layers. The relative frequency of occurrence of these structures is presented for each season and thickness group.

A number of different conceptual models of the stability stratification and shear structure associated with these cloud forms are briefly reviewed. This study attempts to establish (in a quantitative way) the applicability of each of these models for the domain of this analysis.

On a case by case basis, the observed values of the dry static stability, the vertical shear of the horizontal wind speed and the Richardson number may vary over quite large ranges for each layer for either cloud thickness group. The observed stability stratification and vertical wind shear structure about cloud layers is found to be quite variable. Cloud cases exhibiting structures corresponding to each of the different conceptual models may be found in all seasons for both cloud thickness groups. Some structures are found to be substantially more common than others. Some of the observed variability may possibly be explained as arising from errors in locating the actual cloud-top level. These errors may arise due to the differing response rates of the humidity and temperature sensors, (i.e. hysteresis of the humidity sensor may lead to an indication of continuing saturation for a small distance after the sonde has exited the cloud layer). However, the corresponding indicated temperatures and, thus, stability

pertain to the over-cloud layer as the response of the temperature sensor is much faster, especially for these temperatures and pressures.

The major conclusions resulting from these analyses are presented below.

1. In all aspects, the thick cloud cases exhibit larger seasonal variability, than the thin cloud cases. Since cyclone intensity and the associated upper level flow undergo substantial seasonal cycles, it is concluded that the environment of thick middle and upper level cloud forms is much more strongly tied to cyclone intensity than that associated with thin cloud forms.
2. Buoyancy forces are the primary factor influencing the generation of turbulent kinetic energy, and, hence are the primary forces maintaining the vertical transports in middle and upper tropospheric clouds. In only 15–20% of the cloud cases is the mechanical generation, i.e. shear production, of turbulent kinetic energy of equal or greater magnitude. Only rarely is production greater than dissipation of turbulent kinetic energy in the mean flow. Thus, the turbulent energy transports associated with these cloud forms do not result from turbulence maintained by the mean flow.
3. Thick Cloud Layers
  - a. The classical model of the cloud layer existing just above an elevated frontal zone is appropriate for a majority of the thick cloud cases. However, a substantial portion of the cases do not exhibit the very stable sub-cloud layer associated with a front. This may be partly due to problems in locating cloud base or to the

actual extension of the cloud layer below the front due to-precipitation processes occurring in its mature stage.

- b. A majority of the cases, also, exhibit a relatively stable layer in the vicinity of cloud-top. It is not clear whether this feature may be typically explained as a frontal zone or simply due to radiative and evaporative processes occurring in this region.
- c. Well mixed conditions are not commonly observed in any of the three layers, i.e.  $\sim 15\%$  of the cases for either of the layers exhibit a moist adiabatic lapse rate. However, lapse rates within  $1^\circ\text{K}/\text{km}$  to  $2^\circ\text{K}/\text{km}$  of moist adiabatic are typically observed in the cloud-top layer.
- d. The vertical shear of the horizontal wind speed is most commonly a maximum in either the sub-cloud layer or the cloud-top layer. This supports the conclusion that a frontal zone is typically associated with the sub-cloud layer and that a stable capping layer exists in many cases. The structure with maximum vertical shear of the horizontal wind speed occurring in the sub-cloud layer is the mean structure observed.

#### 4. Thin Cloud Layers

a) The typical structure observed for the thin cloud cases does not correspond to the classical model. In fact, the sub-cloud frontal zone is not commonly observed.

b) The over-cloud layer is very stable in a majority of the cases. The observed stability strongly suggests the presence of a frontal zone. However, the potential effects of radiative and evaporative processes could possibly account for this structure. A majority of the cases, which do not exhibit the very stable over-cloud layer, do show a tendency for a weak stability maximum in the vicinity of cloud-top.

c) The cloud-top layer and the sub-cloud layer are found to be very similar in most regards. Approximately 25% of the cases exhibit lapse rates corresponding to near moist adiabatic conditions in these two layers, i. e. the layers are well mixed. Typically, the observed stability of these two layers corresponds to lapse rates within  $1^{\circ}\text{K}/\text{km}$  to  $2^{\circ}\text{K}/\text{km}$  of the moist adiabatic lapse rate.

d) In the mean, vertical wind shear is a maximum in the over-cloud layer though maximum or minimum shears are most commonly observed in the cloud-top layer. A surprising result is that the magnitude of the shear is observed to be larger when negative shear is observed, than when positive shear is observed for each of the layers for the thin cloud cases. We



do not have an explanation of this occurrence. The thick cloud cases show the opposite tendency.

## References

- Albrecht, B. A., A. K. Betts, W. H. Schubert and S. K. Cox, 1979: A model of the thermodynamic structure of the trade-wind boundary layer: Part I. Theoretical formulation and sensitivity tests. J. Atmos. Sci., 36, 73-89.
- Bigg, E. K., and R. T. Meade, 1971: Clear air seeding in the presence of ice supersaturation. Proc. Int. Conf. Wea. Mod. (Canberra, Australia), 141-142.
- Brousaides, F. J., 1973: An assessment of the carbon humidity element in radiosonde systems. Air Force Cambridge Research Laboratories, Instrumentation Papers, No. 197 AFCRL-TR-73-0423, 46 pp.
- \_, and F. J. Morrissey, 1974: Residual temperature-induced humidity errors in the National Weather Service radiosonde, Final Report. Air Force Cambridge Research Laboratories, Instrumentation Papers, No. 215, AFCRL-TR-74-0111, 40 pp.
- Budyko, M. I., 1969: The effects of solar radiation variations on the climate of the earth. Tell us, 21, 611-619.
- Coakley, J. A., Jr., 1979: A study of climate sensitivity using a simple energy balance model. J. Atmos. Sci., 35, 260-269.
- Conover, J., 1960: Cirrus patterns and related air motions near the jet stream as derived by photography. J. Meteor., 17, 532-546.
- Detwiler, A., and B. Vonnegut, 1979: Clear-air seeding. Extended Abstracts 7th Conf. on Inadvertent and Planned Wea. Mod., (Banff, Canada), 15-17.
- Fels, S. B., and L. D. Kaplan, 1975: A test of the role of longwave

radiative transfer in a general circulation model. J. Atmos. Sci.,  
32, 779-789.

Griffith, K. T., S. K. Cox and R. G. Knollenberg, 1979: Infrared  
radiative properties of tropical cirrus clouds inferred from  
aircraft measurements. Submitted for publication to the J. Atmos.  
Sci.

Heymsfield, A. J., 1977: Precipitation development in stratiform ice  
clouds: A microphysical and dynamical study. J. Atmos. Sci., 34  
, 367-381.

International Council of Scientific Unions, 1974: Modelling for the  
First GARP Global Experiment. GARP Publications Series No. 14,  
World Meteorological Organization, 261 pp.

Jayaweera, K.O.L.F., and T. Ohtake, 1972: Artificial cloud formation  
in the atmosphere. Science, 178, 504-505.

Lala, G. G., 1969: Structure and modification of clouds and fogs.  
Ed. by B. Vonnegut, D. C. Blanchard, R. A. Cudney. Research  
Foundation of State University of N.Y., Albany, 84-100.

List, R. J., 1966: Smithsonian Meteorological Tables. Page 370,  
Smithsonian Institution, Washington, D. C., 527 pp.

London, J., 1957: A study of the atmospheric heat balance. Final  
Report, Contract No. AFT9(122)-165, Department of Meteorology  
and Oceanography, New York University, July, 99 pp.

Ludlam, F. H., 1947: The forms of ice clouds. Quart. J. Roy. Met. So.:,  
74, 39-56.

, 1952: Orographic cirrus clouds. Quart. J. Roy. Met.

Soc., 78, 554-562.

Sellers, W. D., 1969: A global climate model based on the energy balance of the earth-atmosphere system. J. Appl. Meteor., 8, 392-400.

Smagorinsky, J., 1960: On the dynamical prediction of large-scale condensation by numerical methods. Geophys. Mono. No. 5, Amer. Geophys. Union, Washington, D. C., 71-78.

Starr, D. O'C., 1976: The sensitivity of tropical radiative budgets to cloud distribution and the radiative properties of clouds. Colorado State University Atmos. Sci. Paper No. 254, NTIS No. PB-263-227, 117 pp.

, and S. K. Cox, 1977: Review of the radiation computations in large scale atmospheric models. Unpublished report available from authors, 26 pp.

Stone, H. M., and S. Manabe, 1968: Comparison among various numerical models designed for computing infrared cooling. Mon. Wea. Rev., 96, 735-741.

U. S. Committee for the Global Atmospheric Research Program, 1978: Elements of the research strategy for the United States Climate Program. National Academy of Sciences, Washington, D. C. 46 pp.

Warren, S. G., and S. H. Schneider, 1979: Seasonal simulation as a test for uncertainties in the parameterizations of a Budyko-Sellers zonal climate model. J. Atmos. Sci., 36, 1377-1391.

Washington, W. M., 1971: On the role of radiation in dynamical climate simulation and numerical weather prediction. Proc. of Miami Workshop on Remote Sensing, 29 - 31 March, Miami, Florida, NOAA, 39-67.

Yagi, T., 1969: On the relation between the shape of cirrus clouds and the static stability of the cloud level. Studies of cirrus clouds: Part IV. J. Meteor. Soc. of Japan, 47, 59-64.

BIBLIOGRAPHIC DATA SHEET	1. Report No. CSU-ATS-327	2.	3. Recipient's Accession No.
4. Title and Subtitle	CHARACTERISTICS OF MIDDLE AND UPPER TROPOSPHERIC CLOUDS AS DEDUCED FROM RAWINSONDE DATA		5. Report Date November, 1980
7. Author(s)	David O'C. Starr and Stephen K. Cox		8. Performing Organization Rept. No. CSU-ATS-327
9. Performing Organization Name and Address	Department of Atmospheric Science Colorado State University Fort Collins, Colorado 80523		10. Project/Task/Work Unit No.
12. Sponsoring Organization Name and Address	National Aeronautics and Space Administration Goddard Space Flight Center Washington, D. C. 20546		11. Contract/Grant No. NSG 5357
			13. Type of Report & Period Covered
15. Supplementary Notes		14.	
<p>16. Abstracts This study characterizes the static environment of middle and upper tropospheric clouds as deduced from rawinsonde data from 24 locations in the contiguous U.S. for 1977. Computed relative humidity with respect to ice is used to diagnose the presence of cloud layer. The deduced seasonal mean cloud cover estimates based on this technique are shown to be reasonable. Over 3600 cloud cases qualified for the analysis. The cases are stratified by season and pressure thickness, i.e. thick and thin. The dry static stability, vertical wind speed shear and Richardson number are computed for three layers for each case, i.e. the sub-cloud and above cloud layers and an in-cloud layer bounded by the cloud-top level. Mean values for each parameter and, in some instances, the corresponding relative frequency distributions are presented for each stratification and layer. The relative frequency of occurrence of various structures is presented for each stratification, e.g. increasing static stability with height through the three layers.</p> <p>The observed values of each parameter vary over quite large ranges for each layer. The observed structure of each parameter for the layers of a given case is also quite variable. Structures corresponding to any of a number of different conceptual models, which are reviewed, may be found though some are substantially more common than others. It is of note that moist adiabatic conditions are not commonly observed and that the stratification based on thickness yields substantially different results for each group. Summaries of the results are included in the text.</p>			
17. Key Words and Document Analysis 17a. Descriptors			
Clouds Ice Clouds Tropospheric cloud characteristics			
17b. Identifiers/Open-Ended Terms			
17c. COSATI Field/Group			
18. Availability Statement	19. Security Class (This Report) UNCLASSIFIED	21. No. of Pages 71	
	20. Security Class (This Page) UNCLASSIFIED	22. Price	